Three-Photon Excitation of Rubidium Atoms to Rydberg States in a Room Temperature Vapor Cell

by

Wei Cui

A thesis
presented to the University of Waterloo
in fulfillment of the
thesis requirement for the degree of
Master of Science
in
Physics

Waterloo, Ontario, Canada, 2016

I hereby declare that I am the sole author of this thesis. This is a true copy of the thesis, including any required final revisions, as accepted by my examiners.

I understand that my thesis may be made electronically available to the public.

Abstract

This thesis presents a method for calculating the absorption of diode lasers in one-photon, two-photon and (Doppler-free) three-photon excitation configurations. The specific three-photon system studied is atomic Rb, $5s_{1/2} - 5p_{3/2} - 5d_{5/2} - np$. In principle three-photon excitation allows for perfect compensation of the Doppler effect. The approach of the method is to construct density matrix equations and solve for the steady state density matrix elements. Solutions are obtained numerically. There is no weak intensity restriction for any laser in the excitation system, and the absorption of all the lasers in the excitation system can be evaluated.

The design and testing of a low-noise transimpedance amplifier for measuring absorption is presented.

Acknowledgements

Dedication

This is dedicated to my father and mother (Zhifeng Cui and Renqing Xu). Thanks for all your support throughout my master program.

Table of Contents

List of Tables

List of Figures

Chapter 1

Introduction

1.1 Motivation

The Doppler-free laser spectroscopy means the wavevectors of the lasers performing the excitation sum to zero. This configuration leads to the Doppler shifts of the frequency of the lasers seen by the atom sum to zero. All the atoms will contribute to the excitation spectroscopy whatever velocity they have, and the resolution of the excitation spectroscopy will be significantly improved. Also, if all the atoms in the cell contribute to the absorption, that means we do not need to build the MOT and other cooling and trapping system to realize the precise measurement. This will save the cost of relevant research.
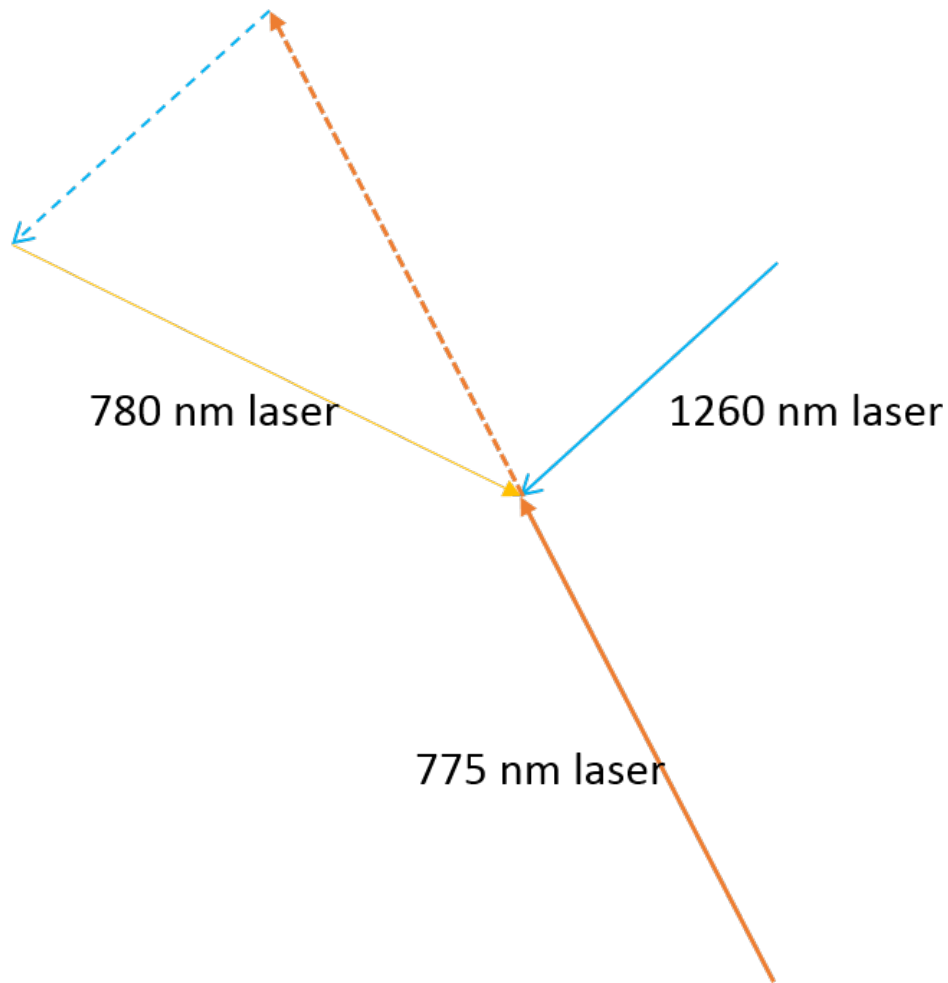
Figure 1.1: 3-photon Doppler-free excitation configuration)

The Doppler-free 3-photon spectroscopy in a Magneto-Optical Trap (MOT) has been studied theoretically applying approximation methods and experimentally [2]. Their result shows that the Doppler-free configuration can eliminate the broadening coming from recoil effect in the spectroscopy. Similar theoretical work for that both in the MOT and room temperature vapor cell has been made [3]. Also, the 3-photon excitation spectroscopy ob-

tained by a collinear configuration has also been experimentally studied [4]. What is more, there are relevant theoretical work about two-photon or three-photon electromagnetically induced transparency [5] [6]. In the EIT paper, the weak probe approximation is applied which means the model constructed is only valid when the probe laser is of low intensity.

At first, we plan to construct a Doppler-free 3-photon excitation in the MOT in our lab. Formerly, the excitation of Rubidium atoms to Rydberg states in the MOT is performed by a 2-photon excitation system in our lab. The energy level relevant with the two excitation configurations in shown in Figure 1.2. The 780 nm laser excites the Rubidium atoms from $5s_{1/2}$ state to $5p_{3/2}$ state. Then the 480 nm laser excites the atoms from $5p_{3/2}$ to $45d_{5/2}$ Rydberg state. There are two main disadvantages of the 2-photon excitation. First, the energy of a photon with 480 nm wavelength is higher than the work function of many metals so applying it near the metal surface in the MOT will cause unexpected photoelectrons which will affect the Rydberg spectroscopy. The second one is the generation of the 480 nm is much more expensive than that of a diode laser [7]. Thus, we planned to construct a Doppler-free 3-photon excitation system in the MOT. In the planned 3-photon excitation system, the $5s_{1/2}$ to $5p_{3/2}$ transition is driven by a 780 nm diode laser and the $5p_{3/2}$ to $5d_{5/2}$ transition is driven by a 775nm diode laser. The last step excitation will be performed by a 1260 nm diode laser exciting the Rubidium atoms from $5d_{5/2}$ to Rydberg states of $n = 50$.
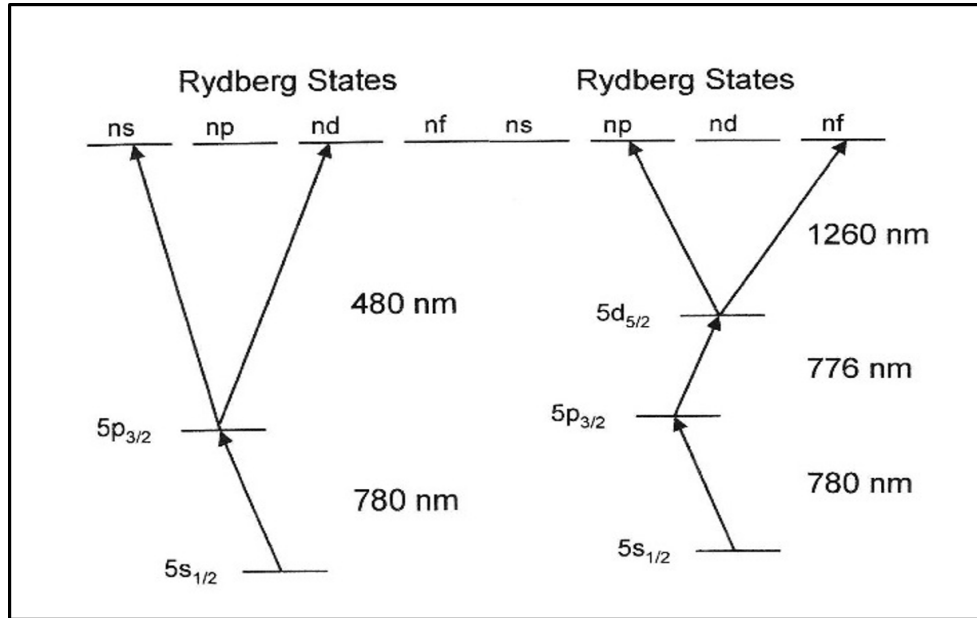
Figure 1.2: Energy levels related to the 2-photon and 3 photon excitation configurations

In the MOT, the atoms are of a temperature near 0 K, which means the Doppler-shift is almost zero. The effect of Doppler-free configuration may not be significant. During the study on Doppler-free spectroscopy technique, I am more and more interested to see how the Doppler-shift is suppressed by the Doppler-free configuration if we perform the excitation in a room temperature cell. Encouraged by my supervisor, I tried to set up a theoretical model which can estimate the absorptions of all the lasers in the Doppler-free 3-photon excitation. All the papers building up the analytical model applied some approximations. Referring to their theory, I used a numerical integration to set up the theoretical model adding as few approximations as possible so there is no limitation of the intensity of the lasers. In this model, the absorption of all the lasers can be estimated, whereas in the analytical model applying the weak probe approximation, only the absorption of a weak intensity probe laser can be calculated.

4

The experimental work for 3-photon excitation has not been finished due to the limitation of time. All the 3 lasers need to be frequency locked. The reason for frequency locking is as following. The energy differences among hyperfine levels in 5d states are from several MHz to tens of MHz. However, the linewidth of the free-running diode laser is around 10MHz. Thus, in order to resolve all the hyperfine levels, we need to have the frequency locked so that the linewidth will be smaller than the energy difference between the hyperfine states [7]. Untill now, I have finished the frequency locking of a 780 nm diode laser using the frequency modulation spectroscopy (FMS) technique. Also, two 775 nm diode lasers have also been frequency locked. One of them is also locked utilizing the FMS technique. This is called static 775 nm laser by us. The other one is lock by the beat -note Pound-Drever-Hall locking technique and we call it dynamic 775 nm diode laser. The linewidth of the three lasers is around 1MHz after being locked. Since there is no data obtained from the experiment, I will focus on the theoretical work in this thesis and the mechanism of the locking technique can be found in the thesis of our former group members such as Ref. [7]. One phenomenon I need to mention is that when the 775 nm laser's frequency is locked, the absorption of the frequency-locked 780 nm laser increased significantly. I thought that is related to the quasi Doppler-free configuration. This is another trigger that made me decide to explore the effect of Doppler-free configuration on the lasers' absorption.

As a part of this project, I designed a transimpedance amplifier which is used to amplify the photocurrent in the FMS system. This amplifier reduced the noise in the FMS signal by 25 times compared with the Former amplifier we used (ZFL-500-BNC [8]). This part work is presented in the Chapter 3.

Chapter 2

Theoretical Work

2.1 Absorption of One-Photon Excitation

The derivations in this section are based on Foot 2013 [9] and Berman 2011 [10].

2.1.1 Beer's Law

Consider a beam of photons passing through an atomic gas. The number density of the atoms in the gas is N_0. A slice of atomic gas of thickness Δz contains $N_0 \Delta z$ every unity area. If we define a quantity σ as the absorption cross-section: fraction of area occupied by atoms in a unity area surface of an atomic slice, which works as a measurement of absorption. Then, The fraction of photons absorbed by the slice of medium can be written as $N_0 \sigma \delta z$. From the statistical point of view $N_0 \sigma \Delta z$ is also the probability that a photon can be absorbed when it passes through an atomic slice.

The intensity loss of the laser beam after going through the atomic slice compared with

the original intensity equals to the probability that a photon can be absorbed:

$$\frac{\Delta I}{I} = -N_0 \sigma \Delta z. \tag{2.1}$$

In the differential form, the absorption can be described as:

$$\frac{dI}{dz} = -a(\omega)I = -N_0\sigma(\omega)I. \tag{2.2}$$

Integrating both sides of Eq. 2.2 gives the Beer's Law:

$$I(\omega, z) = I(\omega, 0)exp(-a(\omega)z). \tag{2.3}$$

Thus, to calculate the absorption of a laser going through an atomic medium, we need to focus on calculating the absorption coefficient $a(\omega)$.

Notice here we write $a(\omega) = N_0\sigma(\omega)$, where N_0 is the number density of atoms in the atomic medium that can interact with the laser field. For the case of one-photon excitation in a 2-level system, the laser field will cause both absorption and stimulated emission. It is known that the cross-section for absorption and that of the stimulated emission are the same [9]. Thus, the N here should be modified to $N_1 - N_2$, where N_1 and N_2 here are the density of atoms in the first and second level of the system. Also we know that $N_1 + N_2 = N_0$.

Then to calculate the value of the absorption cross section, let's consider the steady state of this system. When the 2-level system is in the steady state, the rate that the atoms jump from the ground state to the excited state equals to the rate that the atoms go along the reverse direction. We can also say that the rate of the absorption minus the rate

of the stimulated emission equals to that of the spontaneous decay. Write this combined with the fact that one photon has energy $\hbar\omega$

$$(N_1 - N_2)\sigma(\omega)I(\omega) = N_2\Gamma\hbar\omega, \tag{2.4}$$

where Γ is the rate of the spontaneous decay.

Then we can find that:

$$\sigma(\omega) = \frac{\frac{N_2}{N}}{\frac{N_1-N_2}{N}}\frac{\Gamma\hbar\omega}{I(\omega)}. \tag{2.5}$$

Then in the next section, I will utilize density matrix methods to calculate the value of $\frac{\frac{N_2}{N}}{\frac{N_1-N_2}{N}}$.

2.1.2 Density matrix approach calculating the absorption

Before considering the absorption in the complicated Doppler-free 3-photon excitation, let's first consider the simplest case—the absorption of the laser in a one-photon excitation configuration. This calculation will help us understand the interaction of atoms with radiation.

To illustrate the mechanism, let us start with the time-dependent Schrodinger equation:

$$i\hbar\frac{\partial\psi}{\partial t} = H\psi, \tag{2.6}$$

where the Hamiltonian can be written as:

$$H = H_0 + H_I. \tag{2.7}$$

The H_0 is the Hamiltonian in the absence of the oscillating field and H_I is due to the oscillating field.

An oscillating electric field can be represented as:

$$\mathbf{E} = \mathbf{E}_0 \cos(\omega t). \tag{2.8}$$

Then, the interaction Hamiltonian is:

$$H_I(t) = e\mathbf{r} \cdot \mathbf{E}_0 \cos(\omega t). \tag{2.9}$$

From the theory of quantum mechanics, the spatial wavefunction can be written as:

$$\psi(\mathbf{r}, t) = c_1(t)\psi_1(\mathbf{r})e^{-i\omega_1 t} + c_2(t)\psi_2(\mathbf{r})e^{-i\omega_2 t}, \tag{2.10}$$

where $\hbar\omega_1$ and $\hbar\omega_2$ are the eigenenergies of the two states. The requirement of normalization:

$$|c_1|^2 + |c_2|^2 = 1. \tag{2.11}$$

By plugging Eq. 2.10 into the time-dependent Schrodinger equation Eq. 2.6, we get:

$$i\dot{c}_1 = \Omega \cos(\omega t)e^{-i\omega_0 t}c_2 \tag{2.12a}$$

$$i\dot{c}_2 = \Omega^* \cos(\omega t)e^{i\omega_0 t}c_1, \tag{2.12b}$$

where $\omega_0 = \omega_2 - \omega_1$ and the Ω is the Rabi frequency which is defined as:

$$\Omega = \frac{<1|e\mathbf{r}\cdot\mathbf{E}_0|2>}{\hbar} = \frac{e}{\hbar}\int \psi_1^*(r)\mathbf{r}\cdot\mathbf{E}_0\psi_2(r)d^3\mathbf{r}. \qquad (2.13)$$

For the case where the electric field is almost uniformly distributed in the area of the atomic wave function and the electric field is linearly polarized, the Rabi frequency can be expressed as:

$$\Omega = \frac{eZ_{12}|E_0|}{\hbar}, \qquad (2.14)$$

where:

$$Z_{12} = <1|z|2>, \qquad (2.15)$$

and $|E_0|$ is the amplitude of the electric field.

Note that we also can write equation (3.12) as:

$$i\dot{c}_1 = \frac{\Omega}{2}(e^{i(\omega-\omega_0)t} + e^{-i(\omega+\omega_0)t})c_2 \qquad (2.16a)$$

$$i\dot{c}_2 = \frac{\Omega^*}{2}(e^{i(\omega-\omega_0)t} + e^{-i(\omega+\omega_0)t})c_1. \qquad (2.16b)$$

We can see that the term $+e^{-i(\omega+\omega_0)t}$ is a high-frequency oscillating term. That means from a long-term point of view, this term will average to 0. Dropping these terms is called *rotating-wave approximation*. Then Eq. 2.16 reduces to:

$$i\dot{c}_1 = \Omega e^{i(\omega-\omega_0)t}c_2 \qquad (2.17a)$$

$$i\dot{c}_2 = \Omega^* e^{-i(\omega - \omega_0)t} c_1. \tag{2.17b}$$

Then, the expectation value of the component of the dipole along the polarization direction is:

$$-eD_z(t) = -\int \psi^*(t) ez\psi(t) d^3\mathbf{r}. \tag{2.18}$$

Plugging Eq. 2.10 into Eq. 2.18 yields:

$$D_z = c_2^* c_1 Z_{21} e^{i\omega_0 t} + c_1^* c_2 Z_{12} e^{-i\omega_0 t}. \tag{2.19}$$

Here the $\omega_0 = \omega_2 - \omega_1$. If states 1 and 2 have opposite parity , we know that $Z_{11} = Z_{22} = 0$ [10] and also we know that $Z_{21} = Z_{12}^*$.

Now we need to know the quantities $c_1^* c_2$ and $c_2^* c_1$. These 2 quantities are just 2 of the matrix elements of the density matrix [9].

$$|\psi><\psi| = \begin{pmatrix} c_1 \\ c_2 \end{pmatrix} \begin{pmatrix} c_1^* & c_2^* \end{pmatrix} = \begin{pmatrix} \rho_{11} & \rho_{12} \\ \rho_{21} & \rho_{22} \end{pmatrix}. \tag{2.20}$$

Here the 2 diagonal terms are the population of the atoms in the corresponding energy level. The off-diagonal terms are called coherences [9].

Also, in order to obtain a simpler Hamiltonian of this system, we can write the spatial wave function in a different basis set:

$$|\psi(t)> = \tilde{c}_1(t)|\tilde{1}(t)> + \tilde{c}_2(t)|\tilde{2}(t)>, \tag{2.21}$$

where

$$|\tilde{1}(t)> = e^{i\omega t/2}|1> \tag{2.22a}$$

$$|\tilde{2}(t)> = e^{-i\omega t/2}|2> . \tag{2.22b}$$

This is called the *field interaction representation* [10]. In this basis set, the coefficient before the state kets are:

$$\tilde{\mathbf{c}}(t) = e^{i\delta\boldsymbol{\sigma}_z t/2}\mathbf{c}(t), \tag{2.23}$$

where $\delta = \omega_0 - \omega$.

Here I set $\omega_1 = -\omega_0/2$ and $\omega_2 = \omega_0/2$. Notice that in this basis, the population in each energy level is the same as before:

$$\rho_{nn} = c_n c_n^* = \tilde{c}_n \tilde{c}_n^* = \tilde{\rho}_{nn}, \tag{2.24}$$

and the coherences differ by a phase:

$$\tilde{\rho}_{12} = e^{-i\omega t}\rho_{12} \tag{2.25a}$$

$$\tilde{\rho}_{21} = e^{i\omega t}\rho_{21}. \tag{2.25b}$$

Substituting wavefunction in this basis into the time-dependent Schrodinger equation, we can obtain equations as below:

$$i\hbar\dot{\tilde{\mathbf{c}}} = \tilde{\mathbf{H}}\tilde{\mathbf{c}}, \tag{2.26}$$

12

where the bold c means the vector $\begin{pmatrix} \tilde{c}_1 \\ \tilde{c}_2 \end{pmatrix}$. The $\tilde{H}$ written in matrix form is:

$$\mathbf{\tilde{H}} = \frac{\hbar}{2} \begin{pmatrix} -\delta & \Omega_0(t) \\ \Omega_0(t) & \delta \end{pmatrix}. \tag{2.27}$$

In order to calculate the steady state solution of ρ_{11} and ρ_{22}, we need to set up the density matrix equations:

$$i\hbar d\tilde{\rho}/dt = [\tilde{H}, \tilde{\rho}] + relaxation\, terms. \tag{2.28}$$

Writing the individual elements:

$$\dot{\rho}_{11}(t) = -i\frac{\Omega_0}{2}\tilde{\rho}_{21}(t) + i\frac{\Omega_0}{2}\tilde{\rho}_{12}(t) + \Gamma_2\rho_{22}(t) \tag{2.29a}$$

$$\dot{\rho}_{22}(t) = i\frac{\Omega_0}{2}\tilde{\rho}_{21}(t) - i\frac{\Omega_0}{2}\tilde{\rho}_{12}(t) - \Gamma_2\rho_{22}(t) \tag{2.29b}$$

$$\dot{\tilde{\rho}}_{12}(t) = -i\frac{\Omega_0}{2}\rho_{22} - \rho_{11}) + (i\delta(t) - \Gamma_2/2)\tilde{\rho}_{12}(t) \tag{2.29c}$$

$$\dot{\tilde{\rho}}_{21}(t) = i\frac{\Omega_0}{2}(\rho_{22} - \rho_{11}) + (-i\delta(t) - \Gamma_2/2)\tilde{\rho}_{21}(t), \tag{2.29d}$$

where the Γ_2 is the spontaneous decay rate from the excited state to the ground state. Terms involving Γ_2 are called relaxation terms. In the 2-level system we just take the spontaneous decay into consideration whereas in the future sections when we consider the multi-level system, we will also consider the effect of the linewidth of the lasers. Also, the collision between atoms is another important source of the decay; however, the decay rate caused by the collision between atoms are hard to estimate, and major references in this

13

area always ignore it. In this thesis, we focus on establishing the general theory for laser absorption first, so we ignore the decay rate coming from the collision for now.

In order to get the steady state solutions of the 2-level system, we need to have the derivatives in Eq. 2.29 equal to 0. Also, we know that $\rho11 + \rho_{22}$=1.

Then we just need to solve a set of five simultaneous equations.

$$
\begin{cases}
0 = -i\chi\tilde{\rho}_{21}(t) + i\frac{\Omega_0}{2}\tilde{\rho}_{12}(t) + \Gamma_2\rho_{22}(t) \\
0 = i\chi\tilde{\rho}_{21}(t) - i\frac{\Omega_0}{2}\tilde{\rho}_{12}(t) - \Gamma_2\rho_{22}(t) \\
0 = -i\frac{\Omega_0}{2}(\rho_{22} - \rho_{11}) + (i\delta(t) - \Gamma_2/2)\tilde{\rho}_{12}(t) \\
0 = i\frac{\Omega_0}{2}(\rho_{22} - \rho_{11}) + (-i\delta(t) - \Gamma_2/2)\tilde{\rho}_{21}(t) \\
1 = \rho_{11} + \rho_{22}.
\end{cases}
\tag{2.30}
$$

In this way, the steady state solution of this system can be obtained. What we are interested in are ρ_{22} and $\rho_{11} - \rho_{22}$:

$$
\rho_{22} = \frac{\Omega^2/4}{\delta^2 + \Omega^2/2 + \Gamma^2/4}
\tag{2.31}
$$

$$
\rho_{11} - \rho_{22} = \frac{\delta^2 + \Gamma^2/4}{\delta^2 + \Omega^2/2 + \Gamma^2/4}.
\tag{2.32}
$$

Thus, the absorption coefficient can be calculated (recall Eq. 2.5 in page 5 with $\rho_{22} = \frac{N_2}{N}$ and $\rho_{11} = \frac{N1}{N}$):

$$
\sigma(\omega) = \frac{\rho_{22}}{\rho_{11} - \rho_{22}}\frac{\Gamma\hbar\omega}{I(\omega)} = \frac{\Omega^2/4}{(\omega - \omega_0)^2 + \Gamma^2/4}\frac{\Gamma\hbar\omega}{I}.
\tag{2.33}
$$

Then the absorption coefficient is:

$$
\alpha = (N_1 - N_2)\frac{\Omega^2/4}{(\omega - \omega_0)^2 + \Gamma^2/4}\frac{\Gamma\hbar\omega}{I}.
\tag{2.34}
$$

14

Combining Eq. 2.4 with the fact $N_1 + N_2 = N$, we can get:

$$N_1 - N_2 = \frac{N}{1 + 2r} = \frac{N}{1 + I/I_s(\omega)}, \tag{2.35}$$

where:

$$r = \frac{\hbar \omega \Gamma}{2\sigma \omega}, \tag{2.36}$$

and:

$$I_s(\omega) = \frac{\hbar \omega \Gamma}{2\sigma(\omega)}. \tag{2.37}$$

From section 7.2 in Foot (2013), we can get that:

$$\Gamma = \frac{4\alpha \omega^3 X_{12}^2}{3c^2} \tag{2.38}$$

Then expression of the cross-section can be written out as:

$$\sigma(\omega) = \frac{\pi^2 c^2}{\omega_0^2} \frac{1}{2\pi} \frac{\Gamma^2}{(\omega - \omega_0)^2 + \Gamma^2/4} \tag{2.39}$$

The equations here is under the assumption that the frequency of the laser field ω is near the resonant frequency ω_0 (the ω_0^2 is approximated from ω^2 in the derivation).

The last step of this estimation is to take the Doppler-effect into consideration. The Doppler effect will influence the frequency of the photon seen by the atoms. Thus, we can take the Doppler effect into consideration by changing ω to $\omega - kv$ in the expression of absorption cross-section and absorption coefficient. At last, we need to take the Maxwell

distribution of the atoms' velocity into account and integrate the product of the velocity distribution function and the absorption coefficient over all the possible velocities.

Thus,

$$\sigma(\omega - kv) = \frac{\pi^2 c^2}{2\pi\omega_0^2} \frac{\Gamma^2}{(\omega - \omega_0 - kv)^2 + \Gamma^2/4}. \tag{2.40}$$

and

$$\alpha(\omega - kv) = \frac{N\sigma(\omega - kv)}{1 + \frac{I}{\hbar\omega\Gamma/(2\sigma(\omega - kv))}}, \tag{2.41}$$

Finally,

$$\alpha = \int_{-\infty}^{+\infty} f(v)\alpha(\omega - kv)dv, \tag{2.42}$$

where $f(v) = \frac{1}{u\sqrt{\pi}}exp(-v^2/u^2)$ and u is the most probable speed $(u = \sqrt{\frac{2k_B T}{M}})$.

Here, an example of the absorption of a 780 nm laser in a 12 cm long Rubidium cell at room temperature (300 K) is presented.

From Steck (2015) [11], the vapor pressure of Rubidium 87 atoms is $3.92 \times 10^{-7} torr$ which equals to $5.225 \times 10^{-5} Pa$. Then utilizing the ideal gas law $PV = NkT$, we can calculate the atom density in the room temperature cell:

$$n = \frac{N}{V} = \frac{P}{kT} = \frac{5.225 \times 10^{-5} kg m^{-1} s^{-2}}{1.38 \times 10^{-23} JK^{-1} \times 300K} = 1.26 \times 10^{16}/m^3. \tag{2.43}$$

From the statistical mechanics, we know that the most probable speed is:

$$u = \sqrt{\frac{2k_B T}{M}} = 239 ms^{-1}. \tag{2.44}$$

16

Then, by plugging in all the variables into the equation (3.50), we can calculate the absorption coefficient as:

$$\alpha = \int_{-\infty}^{+\infty} \frac{1}{u\sqrt{\pi}} exp(-v^2/u^2) \frac{N\frac{\pi^2 c^2}{2\pi\omega_0^2}\frac{\Gamma^2}{(\omega-\omega_0-kv)^2+\Gamma^2/4}}{1+\frac{I}{\hbar\omega\Gamma/(2\frac{\pi^2 c^2}{2\pi\omega_0^2}\frac{\Gamma^2}{(\omega-\omega_0-kv)^2+\Gamma^2/4})}} dv. \tag{2.45}$$

Substitute all the physical constants and related parameters of the 5s to 5p transition of Rb 87 into Eq. **??** and we will get the absorption coefficient. Here the absorption coefficient equals to $11.681 m^{-1}$.

Some of the parameters are listed as below[12]:

$$\Gamma = 5.89 \times 10^6 \times 2\pi$$

$$\Omega/\Gamma = (I/7.56mW\,cm^{-2})$$

The ratio of laser intensity after the laser passes through the atomic cell is:

$$T = e^{-\alpha x} = e^{-11.681 \times 0.12} = 24.6\% \tag{2.46}$$

This is comparable to what is observed in practice.

2.2   Absorption in a 2-photon excitation system

2.2.1   Complex Susceptibility

The 2-photon excitation occurs in a 3-level ladder system. Here for the Rb 87 atoms, the three levels are $5s_{1/2}$, $5p_{3/2}$ and $5d_{5/2}$ individually. The wavelength of the laser driving the first transition is 780.234 nm and we call this laser pumping laser. The wavelength of the laser driving the second transition is 775.975 nm and is called probe laser here.

Unlike the 1-photon excitation case, it is hard to find an expression of the absorption cross-section here. Thus, we need to find out another method to obtain the expression of the absorption coefficient. Here I introduce the method determining the absorption coefficient through calculating the complex susceptibility. This section is based on the doctoral thesis of Dr. Purve (2006) [13].

Let's first consider a medium with N oscillators per unit volume. Each oscillator has a dipole moment $\mathbf{d}$. Then the total polarization $\mathbf{P}$ of the medium can be written as:

$$\mathbf{P} = N < \mathbf{d} >, \tag{2.47}$$

where the $< \mathbf{d} >$ means the expectation value of the dipole moment.

From quantum mechanics, we know that:

$$< \mathbf{d} >= Tr(\rho \mathbf{d}), \tag{2.48}$$

where the ρ is the density matrix.

Since the medium is in the electric field, the polarization can also be written as:

$$\mathbf{P} = \frac{1}{2}\epsilon_0\mathbf{E}_{pr}(\chi e^{i\omega_{pr}t} + \chi^*e^{-i\omega_{pr}t}), \tag{2.49}$$

where the χ is the complex susceptibility of the medium.

Here I will take the 3-level system mentioned at the beginning of this section as an example. The dipole moment in the matrix form is written as:

$$\mathbf{d} = \begin{pmatrix} 0 & \mathbf{d}_{12} & 0 \\ \mathbf{d}_{21} & 0 & \mathbf{d}_{23} \\ 0 & \mathbf{d}_{32} & 0 \end{pmatrix}. \tag{2.50}$$

Then the polarization becomes:

$$\mathbf{P} = \frac{1}{2}\epsilon_0\mathbf{E}_{pu}(\chi e^{i\omega_{pu}t} + \chi^*e^{-i\omega_{pu}t}) + \frac{1}{2}\epsilon_0\mathbf{E}_{pr}(\chi e^{i\omega_{pr}t} + \chi^*e^{-i\omega_{pr}t}). \tag{2.51}$$

The density matrix is just:

$$\rho = \begin{pmatrix} \rho_{11} & \rho_{12} & \rho_{13} \\ \rho_{21} & \rho_{22} & \rho_{23} \\ \rho_{31} & \rho_{32} & \rho_{33} \end{pmatrix}, \tag{2.52}$$

and,

$$\rho\mathbf{d} = \begin{pmatrix} \mathbf{d}_{21}\rho_{12} & \mathbf{d}_{12}\rho_{11} + \mathbf{d}_{32}\rho_{13} & \mathbf{d}_{32}\rho_{21} \\ \mathbf{d}_{21}\rho_{22} & \mathbf{d}_{12}\rho_{21} + \mathbf{d}_{32}\rho_{23} & \mathbf{d}_{23}\rho_{22} \\ \mathbf{d}_{21}\rho_{32} & \mathbf{d}_{12}\rho_{31} + \mathbf{d}_{32}\rho_{33} & \mathbf{d}_{23}\rho_{32} \end{pmatrix}. \tag{2.53}$$

Then the expectation value of the dipole moment is:

$$< \mathbf{d} >= Tr(\rho \mathbf{d}) = \mathbf{d}_{21}(\rho_{12} + \rho_{21}) + \mathbf{d}_{32}(\rho_{32} + \rho_{23}). \tag{2.54}$$

Noticing from quantum mechanics, if we define the polarization direction as the direction of the z-axis, the matrix element $\mathbf{d}_{mn}$ will be a real number so we have $\mathbf{d}_{21} = \mathbf{d}_{12}$. Also we assume that the polarization direction of the 2 lasers here is the same.

As introduced in section 3.1, if we write everything in the field interaction representation:

$$< \mathbf{d} >= \mathbf{d}_{21}(\tilde{\rho}_{12}e^{i\omega_{pu}t} + \tilde{\rho}_{21}e^{-i\omega_{pu}t}) + \mathbf{d}_{32}(\tilde{\rho}_{32}e^{-i\omega_{pr}t} + \tilde{\rho}_{23}e^{i\omega_{pr}t}). \tag{2.55}$$

Thus, we can write the polarization as:

$$\mathbf{P} = N(\mathbf{d}_{21}(\tilde{\rho}_{12}e^{i\omega_{pu}t} + \tilde{\rho}_{21}e^{-i\omega_{pu}t}) + \mathbf{d}_{32}(\tilde{\rho}_{32}e^{-i\omega_{pr}t} + \tilde{\rho}_{23}e^{i\omega_{pr}t})). \tag{2.56}$$

Combining Eq. 2.51 and Eq. 2.56 and equating the terms with the frequency $e^{-i\omega_{pr}t}$, we can get:

$$\frac{1}{2}\epsilon_0 \mathbf{E}_{pr}\chi^* e^{-i\omega_{pr}t} = N\mathbf{d}_{32}\tilde{\rho}_{32}e^{-i\omega_{pr}t}. \tag{2.57}$$

Thus, the relationship between complex susceptibility and specific density matrix element is given by:

$$\chi = -\frac{2Nd_{32}^2}{\epsilon_0 \hbar \Omega_{pr}}\tilde{\rho}_{32}. \tag{2.58}$$

The real and imaginary part of the complex susceptibility corresponds to the dispersion and absorption characters of the atomic vapor [14]. The relationship between the imaginary part of the complex susceptibility and the absorption coefficient can be written as:

$$\alpha = k_p Im[\chi]. \tag{2.59}$$

Thus, as long as we can find out the expression of the corresponding density matrix elements (coherences), we will be able to estimate the absorption of the laser traveling through the atomic medium.

In the next 2 sections, I will present an analytical method and a numerical method to solve the density matrix equations for the steady state solution of the density matrix elements corresponding to coherences.

2.2.2 Apply a Perturbation Technique to Solve for the Steady State Solution

Before writing out the density matrix equations, we need to make it clear that the density matrix elements related to the complex susceptibility in Eq. 2.58 are written in the field interaction representation. Thus, we need to write the density matrix equations in the field interaction representation. We can utilize Eq. 2.28 $i\hbar d\tilde{\rho}/dt = [\tilde{H}, \tilde{\rho}] + relaxation\,terms$ to write out the density matrix equations for the 3-level system.

Let's first write out the basis for the field interaction representation:

$$|\tilde{1}(t)> = e^{i\omega_{pu}t}|1> \tag{2.60a}$$

$$|\tilde{2}(t)> = |2> \tag{2.60b}$$

$$|\tilde{3}(t)> = e^{-i\omega_{pr}t}|3> . \tag{2.60c}$$

Here we set the energy of the second energy level as 0.

Plug $|\psi(t)> = \sum \tilde{c}_n|n(t)>$ into the time dependent Schrodinger equation and then we will get a set of equations that can be written in the vector form.

$$i\hbar\dot{\tilde{\mathbf{c}}} = \tilde{\mathbf{H}}\tilde{\mathbf{c}}. \tag{2.61}$$

In this way, the form of the Hamiltonian written in the field interaction representation can be written out as:

$$\tilde{\mathbf{H}} = \begin{pmatrix} -\delta_{pu} & \frac{\Omega_{pu}}{2} & 0 \\ \frac{\Omega_{pu}}{2} & 0 & \frac{\Omega_{pr}}{2} \\ 0 & \frac{\Omega_{pr}}{2} & \delta_{pr} \end{pmatrix} . \tag{2.62}$$

Then, we can apply the equation (3.33) to write out the density matrix equations in the field interaction representation:

$$\dot{\rho}_{00} = i\Omega_{pu}(\tilde{\rho}_{01} - \tilde{\rho}_{10}) + \Gamma_1\rho_{11} \tag{2.63a}$$

$$\dot{\rho}_{11} = i\Omega_{pu}(\tilde{\rho}_{10} - \tilde{\rho}_{01}) + \Omega_{pr}(\tilde{\rho}_{12} - \tilde{\rho}_{21}) + \Gamma_2\rho_{22} - \Gamma_1\rho_{11} \tag{2.63b}$$

$$\dot{\rho}_{22} = i\Omega_{pr}(\tilde{\rho}_{21} - \tilde{\rho}_{12}) - \Gamma_2\rho_{22} \tag{2.63c}$$

$$\dot{\tilde{\rho}}_{01} = i\frac{\Omega_{pu}}{2}(\rho_{00} - \rho_{11}) + i\frac{\Omega_{pr}}{2}\tilde{\rho}_{02} - (i\Delta_{pu} + \gamma_{01})\tilde{\rho_{01}} \tag{2.63d}$$

$$\dot{\tilde{\rho}}_{12} = i\frac{\Omega_{pr}}{2}(\rho_{11} - \rho_{22}) - i\frac{\Omega_{pu}}{2}\tilde{\rho}_{02} - (i\Delta_{pr} + \gamma_{12})\tilde{\rho_{12}} \tag{2.63e}$$

$$\dot{\tilde{\rho}}_{02} = i\frac{\Omega_{pr}}{2}\rho_{01} - i\frac{\Omega_{pu}}{2}\tilde{\rho}_{12} - (i(\Delta_{pu} + \Delta_{pr}) + \gamma_{02})\tilde{\rho}_{02}, \tag{2.63f}$$

where $\gamma_{01} = \Gamma_1/2 + \gamma_{pu}$, $\gamma_{12} = (\Gamma_1 + \Gamma_2)/2 + \gamma_{pr}$ and $\gamma_{01} = \Gamma_2/2 + \gamma_{pu} + \gamma_{pr}$. The Γ's here are the spontaneous decay rates for corresponding states. γ_{pu} and γ_{pr} are the dephasing terms caused by the linewidth of the pump and probe laser here [6]. Note that in this set of density matrix equations, we left out the three equations for $\dot{\tilde{\rho}}_{10}$, $\dot{\tilde{\rho}}_{21}$ and $\dot{\tilde{\rho}}_{31}$. That is because they are just the complex conjugate of Eq. (2.63d), Eq. (2.63e), and Eq. (2.63f)

Now, let's find out the steady state solution for the density matrix equations here. The same with that in a 2-level system, we just need to set all the derivatives in the density matrix equations equal to 0 and combine them with the equation $\rho_{11} + \rho_{22} + \rho_{33} = 1$.

Then we will have to solve this 10 simultaneous equations for the steady state of $\tilde{\rho}_{21}$ here. If we directly solve the 10 equations analytically, the result will be extremely complicated. Remembering that to consider the Doppler effect, we need to change the detune of the lasers from Δ to $\Delta + \mathbf{k} \cdot \mathbf{v}$ and then integrate the expression of the absorption coefficient over the

whole velocity range. Since the expression of the steady state solution is too complicated to be analytically integrated, we need to make some approximations to get a analytical result or get a numerical result with the help of some software such as Mathematica.

In this section, I will apply a perturbation method to get an approximated expression of the absorption coefficient. The following material is basically following the paper by M. Tanasittikosol [6].

Let's first introduce the precondition for the perturbation method: $\Omega_{pr}/\gamma_{12} \ll 1$. This is called *weak probe condition*. The Rabi frequency of this transition much less than the relaxation terms means the rate the atoms are excited is much less than that of the spontaneous decay rate. Thus, the probe laser will merely affect the population of the excited state in the transition it couples.

As long as the Rabi frequency here is a small value here, we can always expand the density matrix in the power of Ω_{pr} :

$$\tilde{\rho}_{ij} = \tilde{\rho}_{ij}^{(0)} + \tilde{\rho}_{ij}^{(1)}\Omega_{pr} + \tilde{\rho}_{ij}^{(2)}\Omega_{pr}^2 + \tilde{\rho}_{ij}^{(3)}\Omega_{pr}^3 + \cdots, \tag{2.64}$$

where the $\tilde{\rho}_{ij}^{(n)}$ means the nth order of correction of $\tilde{\rho}_{ij}$ in its expansion.

Next step is to substitute the Eq. 2.64 into the density matrix equations (Eq. 2.63) and equating the terms with the same power of Ω_{pr}. The equations coming from the terms with zeroth power of Ω_{pr} are:

$$\Gamma_1 \rho_{11}^{(0)} + \frac{1}{2}\Omega_{pu}(\tilde{\rho}_{01} - \tilde{\rho}_{10}) = 0 \tag{2.65a}$$

$$\Gamma_2 \rho_{22}^{(0)} = 0 \tag{2.65b}$$

$$(i\Delta_{pu} + \gamma_{01})\tilde{\rho}_{01}^{(0)} + \frac{i}{2}\Omega_{pu}(\rho_{11}^{(0)} - \rho_{00}^{(0)}) = 0 \tag{2.65c}$$

24

$$(i\Delta_{pr} + \gamma_{12}))\tilde{\rho}_{12}^{(0)} + \frac{i}{2}\Omega_{pu}\tilde{\rho}_{02}^{(0)} = 0 \tag{2.65d}$$

$$(i\Delta_r + \gamma_{02}))\tilde{\rho}_{02}^{(0)} + \frac{i}{2}\Omega_{pu}\tilde{\rho}_{12}^{(0)} = 0 \tag{2.65e}$$

$$\rho_{00}^{(0)} + \rho_{11}^{(0)} + \rho_{22}^{(0)} = 1, \tag{2.65f}$$

where the $\Delta_r = \Delta_{pu} + \Delta_{pr}$.

From Eq. 2.65, we can find that $\rho_{22} = \tilde{\rho}_{12} = 0$, the expressions for the nonzero density matrix elements are:

$$\tilde{\rho}_{01}^{(0)} = \frac{i\Omega_{pu}}{2}[\gamma_{01} + i\Gamma_{pu} + \frac{\Omega_{pu}^2\gamma_{01}}{(\gamma_{01} - i\Gamma_{pu})\Gamma_1}]^{-1} \tag{2.66}$$

$$\rho_{11}^{(0)} = \frac{\Omega_{pr}^2\gamma_{01}/2}{\Gamma_1\Delta_{pu}^2 + \Gamma_1\gamma_{01}^2 + \gamma^{01}\Omega_{pu}^2} \tag{2.67}$$

,

and $\rho_{00}^{(0)} = 1 - \rho_{11}^{(0)}$.

Similarly, the equations for higher power (for $n \geqslant 1$)of Ω_{pr} can be written as:

$$\Gamma_1\rho_1^{(n)}1 + \frac{i}{2}\Omega_c(\tilde{\rho}_{01}^{(n)} - \tilde{\rho}_{10}^{(n)}) = 0 \tag{2.68a}$$

$$\Gamma_2\rho_2^{(n)}2 + \frac{i}{2}(\tilde{\rho}_{12}^{(n-1)} - \tilde{\rho}_{21}^{(n-1)}) = 0 \tag{2.68b}$$

$$(i\Delta_{pu} + \gamma_{01}\tilde{\rho}_{01}^{(n)}) - \frac{i}{2}\tilde{\rho}_{02}^{(n-1)} + \frac{i}{2}\Omega_{pu}(\rho_{11}^{(n)} - \rho_{00}^{(n)}) = 0 \tag{2.68c}$$

$$(i\Delta_{pr} + \gamma_{02}\tilde{\rho}_{12}^{(n)}) + \frac{i}{2}\Omega_{pu}\tilde{\rho}_{02}^{(n)} + \frac{i}{2}(\rho_{22}^{(n-1)} - \rho_{11}^{(n-1)}) = 0 \tag{2.68d}$$

$$(i\Delta r + \gamma_{12})\tilde{\rho}_{02}^{(n)} - \frac{i}{2}\tilde{\rho}_{01}^{(n-1)} + \frac{i}{2}\Omega_c\tilde{\rho}_{12}^{(n)} \tag{2.68e}$$

$$\rho_{00}^{(n)} + \rho_{11}^{(n)} + \rho_{22}^{(n)} = 0. \tag{2.68f}$$

Combining Eq. 2.66, Eq. 2.67 and Eq. 2.68, we will find that all the $\tilde{\rho}_{ij}^{(1)}$'s equals to 0 except $\tilde{\rho}_{02}^{(1)}$ and $\tilde{\rho}_{12}^{(1)}$. The expressions of $\tilde{\rho}_{02}^{(1)}$ and $\tilde{\rho}_{12}^{(1)}$ are:

$$\tilde{\rho}_{02}^{(1)} = \frac{2\Gamma_1(i\Delta_{pr} + \gamma 02)(i\Delta_{pu} - \gamma_{01})\Omega_{pu} + \gamma_{01}\Omega_{pu}^3}{2(\Gamma_1\Delta_{pu}^2 + \Gamma_1\gamma_{01}^2 + \gamma_{01}\Omega_{pu})[4(i\Delta_{pr} + \gamma_{02})(i\Delta_r + \gamma_{12}) + \Omega_{pu}^2]} \quad (2.69)$$

$$\tilde{\rho}_{12}^{(1)} = \frac{i\Omega_{pu}^2\gamma_{01}}{4(\Gamma_1\Delta_{pu}^2 + \Gamma_1\gamma_{01}^2 + \gamma_{01}\Omega_{pu}^2)}[1 + \frac{\gamma_{pu}(1 + i\Delta_{pu}/\gamma_{01})}{\gamma_{02} + i\gamma_{pr}}][\gamma_{12} + i\Delta_r + \frac{\Omega_{pu}^2}{4(\gamma_{02} + i\gamma_{pr})}]^{-1}. \quad (2.70)$$

These are the first order correction terms of the density matrix elements. Then, based on the zeroth order and first order correction terms, we can solve for the second order correction of the density matrix elements. From calculation we can show that $\tilde{\rho}_{12}^{(2)} = \tilde{\rho}_{02}^{(2)} = 0$.

Thus, we have got the coherence up to the second order corrections:

$$\tilde{\rho}_{02} = \Omega_{pr}\tilde{\rho}_{02}^{(1)} = \frac{2\Gamma_1(i\Delta_{pr} + \gamma 02)(i\Delta_{pu} - \gamma_{01})\Omega_{pu}\Omega_{pr} + \gamma_{01}\Omega_{pu}^3\Omega_{pr}}{2(\Gamma_1\Delta_{pu}^2 + \Gamma_1\gamma_{01}^2 + \gamma_{01}\Omega_{pu})[4(i\Delta_{pr} + \gamma_{02})(i\Delta_r + \gamma_{12}) + \Omega_{pu}^2]} \quad (2.71)$$

$$\tilde{\rho}_{12} = \Omega_{pr}\tilde{\rho}_{12}^{(1)} = \frac{i\Omega_{pu}^2\Omega_{pr}\gamma_{01}}{4(\Gamma_1\Delta_{pu}^2 + \Gamma_1\gamma_{01}^2 + \gamma_{01}\Omega_{pu}^2)}[1 + \frac{\gamma_{pu}(1 + i\Delta_{pu}/\gamma_{01})}{\gamma_{02} + i\gamma_{pr}}][\gamma_{12} + i\Delta_r + \frac{\Omega_{pu}^2}{4(\gamma_{02} + i\gamma_{pr})}]^{-1}. \quad (2.72)$$

Then we can write out the absorption coefficient for the 775nm laser:

$$\chi = -\frac{2Nd_{21}^2\tilde{\rho}_{21}}{\hbar\epsilon_0\Omega_{pr}} = -\frac{2Nd_{21}^2\tilde{\rho}_{21}^{(1)}}{\hbar\epsilon_0} \quad (2.73a)$$

$$\alpha = k_{pr}Im[\chi]. \quad (2.73b)$$

In this particular case, we know that the population of the 5P state is resonantly pumped from 5S state. Thus, $\Delta_{pu} \approx 0$ and also $\gamma_{pu} \ll \gamma_{01}$. According to these, we can

approximately consider the second bracket in the expression of $\tilde{\rho}_{12}$ to be unity. Therefore, we have:

$$\tilde{\rho}_{12} = \frac{i\Omega_{pu}^2 \Omega_{pr}\gamma_{01}}{4(\Gamma_1\Delta_{pu}^2 + \Gamma_1\gamma_{01}^2 + \gamma_{01}\Omega_{pu}^2)}[\gamma_{12} + i\Delta_r + \frac{\Omega_{pu}^2}{4(\gamma_{02} + i\gamma_{pr})}]^{-1}. \tag{2.74}$$

Till now, we have finished the evaluation of the absorption coefficient if all the atoms are stationary in the cell. Next, we need to take the motion of the atoms in the cell into consideration. The same as the calculation in the 2-level system, the motion of the atoms causes the Doppler shift and is presented in the detuning of 2 lasers:

$$\Delta pr \to \Delta pr - k_{pr}v \tag{2.75}$$

$$\Delta pu \to \Delta pu + k_{pr}v, \tag{2.76}$$

and the Maxwell distribution is:

$$N \to \frac{N}{u\sqrt{\pi}}exp(-\frac{v^2}{u^2}). \tag{2.77}$$

Same as before, the u here is the most probable speed of atoms moving in the cell at a given temperature T. Notice here the symbol of the Doppler shift in the 2 detuning terms are different That is because the 2 lasers beam are counter-propagating with each other. Let's consider a portion of atoms with almost the same velocity. The frequency of one of the lasers seen by these atoms will be up shifted and that of the other laser seen by these atoms will be down shifted.

Then substitute Eq. 2.75, Eq. 2.76, and Eq. 2.77 into the Eq. 2.74 and do some modification:

$$\chi(v)dv = -\frac{Nd_{21}^2\Omega_{pu}^2}{\hbar\epsilon_0\sqrt{\pi}k_{pu}^2(k_{pu}-k_{kp})u^3}\frac{\gamma_{01}}{2\Gamma_1}[\frac{e^{-z^2}}{(z+\beta)^2+\sigma^2}][z-z_0+\frac{\Omega_{pu}^2/4}{(k_{pu}-k_{pr})k_{pr}u^2(z-z_1)}]^{-1},$$

$$(2.78)$$

where:

$$\gamma = \frac{\gamma_{12}}{(k_{pu}-k_{pr})u} \qquad (2.79a)$$

$$\sigma = \frac{1}{(k_{pu}-k_{pr})u} \qquad (2.79b)$$

$$\xi = \frac{\Delta_r}{(k_{pu}-l_{pr})u} \qquad (2.79c)$$

$$\beta = \frac{\Delta_{pu}}{k_{pu}u} \qquad (2.79d)$$

$$z_0 = -\xi - i\gamma \qquad (2.79e)$$

$$z_1 = \frac{\Delta_{pr}+i\gamma_{01}}{k_{pr}u}. \qquad (2.79f)$$

The total susceptibility is the integration of equation (3.78) over the whole velocity range:

$$\chi(\Delta_{pr}) = -\frac{Nd_{21}^2\Omega_{pu}^2}{\bar{\epsilon}\sqrt{pi}k_{pu}^2(k_{pu}-k_{pr})u^3}\frac{\gamma_{01}}{2\Gamma_1}\int_{-\infty}^{+\infty}[\frac{e^{-z^2}}{(z+\beta)^2+\sigma^2}][z-z_0+\frac{\Omega_{pu}^2/4}{(k_{pu}-k_{pr})k_{pr}u^2(z-z_1)}]dz.$$

$$(2.80)$$

The expression out of the integration is a constant. Thus, the only part we need to consider is the integrand:

$$\int_{-\infty}^{+\infty}\frac{e^{(-z^2)}}{(z+\beta)^2+\sigma^2}[z-z_0+\frac{\Omega_{pu}^2/4}{(k_{pu}-k_{pr})k_{pr}u^2(z-z_1)}]^{-1}. \qquad (2.81)$$

We can use the partial fractions as:

$$
\frac{e^{-z^2}}{(z+\beta)^2+\sigma^2}[z-z_0+\frac{\Omega_{pr}^2/4}{(k_{pu}-k_{pr})k_{pr}u^2(z-z_1)}]^{-1}
$$
$$
= -\frac{z-z_1}{[(\beta+\phi_+)^2+\sigma^2](\phi_+-\phi_-)}\frac{e^{-z^2}}{z-\phi_+}
$$
$$
+\frac{z-z_1}{[(\beta+\phi_-)^2+\sigma^2](\phi_+-\phi_-)}\frac{e^{-z^2}}{z-\phi_-}
$$
$$
-\frac{i(z-z_1)}{2\sigma(\beta+\phi_++i\sigma)(\beta+\phi_-+i\sigma)}\frac{e^{-z^2}}{z+\beta+i\sigma}
$$
$$
+\frac{i(z-z_1)}{2\sigma(\beta+\phi_+-i\sigma)(\beta+\phi_--i\sigma)}\frac{e^{-z^2}}{z+\beta-i\sigma}
$$

(2.82)

,

where:

$$
\phi_\pm = \frac{1}{2}(z_0+z_1)\pm\frac{1}{2}\sqrt{(z_0-z_1)^2-\frac{\Omega_c^2}{k_{pr}(k_{pu}-k_{pr})u^2}}.
$$

(2.83)

Notice the property:

$$
\int_{-\infty}^{+\infty}\frac{e^{-z^2}(z-a)}{z-b}dz = -(a-b)\int_{-\infty}^{+\infty}\frac{e^{-z^2}}{z-b}+\sqrt{\pi}.
$$

(2.84)

Then, the equation (3.82) can be written as:

$$\frac{e^{-z^2}}{(z+\beta)^2+\sigma^2}[z-z_0+\frac{\Omega_{pr}^2/4}{(k_{pu}-k_{pr})k_{pr}u^2(z-z_1)}]^{-1}$$

$$= -\frac{z_1-\phi_+}{[(\beta+\phi_+)^2+\sigma^2](\phi_+-\phi_-)}\frac{e^{-z^2}}{z-\phi_+}$$

$$+\frac{z_1-\phi_-}{[(\beta+\phi_-)^2+\sigma^2](\phi_+-\phi_-)}\frac{e^{-z^2}}{z-\phi_-} \tag{2.85}$$

$$-\frac{i(z_1+\beta+i\sigma)}{2\sigma(\beta+\phi_++i\sigma)(\beta+\phi_-+i\sigma)}\frac{e^{-z^2}}{z+\beta+i\sigma}$$

$$+\frac{i(z_1+\beta-i\sigma)}{2\sigma(\beta+\phi_+-i\sigma)(\beta+\phi_--i\sigma)}\frac{e^{-z^2}}{z+\beta-i\sigma}$$

Looking at the form of equation (3.85), the form of the integral need to be evaluated is:

$$\int_{-\infty}^{+\infty}\frac{e^{-z^2}}{z-z_p}dz \tag{2.86}$$

The solution of the integration is given by:

$$\int_{-\infty}^{+\infty}\frac{e^{-z^2}}{z-z_p}dz = is\pi W(sz_p) \tag{2.87}$$

where $s = sgn[Im(z_p)]$ is the signum function. Its value is $+1$ when z_p is positive, and -1 when z_p is negative. The W(z) is the Faddeeva function [15] which is defined as:

$$W(z) = e^{-z^2}erfc(-iz) \tag{2.88}$$

and the erfc function is the complex error function. Its definition is:

$$erfc(z) = 1 - erf(z) = \frac{2}{\sqrt{\pi}}\int_z^\infty e^{-t^2}dt \tag{2.89}$$

30

The erf function is the well-known error function.

Thus, the total complex susceptibility is:

$$
\begin{aligned}
\chi_D = {} & -\frac{iNd_{21}^2\Omega_{pu}^2}{\hbar\epsilon_0 k_{pu}^2(k_{pu}-k_{pr})u^3}\frac{\gamma_{01}}{2\Gamma_1} \\
& \times [-\frac{z_1-\phi_+}{[(\beta+\phi_+)^2+\sigma^2](\phi_+-\phi_-)}s_+W(s_+\phi_+) \\
& +\frac{z_1-\phi_-}{[(\beta+\phi_-)^2+\sigma^2](\phi_+-\phi_-)}s_-W(s_-\phi_-) \\
& +\frac{i(z_1+\beta+i\sigma)}{2\sigma(\beta+\phi_++i\sigma)(\beta+\phi_-+i\sigma)}W(+\beta+i\sigma) \\
& +\frac{i(z_1+\beta-i\sigma)}{2\sigma(\beta+\phi_+-i\sigma)(\beta+\phi_--i\sigma)}W(-\beta-i\sigma) \\
& .
\end{aligned}
\tag{2.90}
$$

where $s_+ = sgn[Im(\phi_+)]$ and $s_- = sgn[Im(\phi_-)]$.

Here I made two corrections on the Eq. B7 in Ref. [6]. The sign before the third term should be $+$ instead of $-$. Also, in the denominator of third term, it should be $z+\beta+i\sigma$ instead of $z-\beta-i\sigma$.

To this point, we just need to substitute all the value of the parameters in Eq. 2.90. Here I set the 775 nm laser' intensity as 1 mW/cm^2, which fits the weak probe condition. From Eq. 2.73b we will get the expression of the absorption coefficient. We know that the transmission coefficient is

$$
T = e^{-\alpha z},
\tag{2.91}
$$

where z is the distance within which the laser interacts with the atoms.

Then plot the relationship between the transmission coefficient T and Δ_{pr}. The plot is in figure 3.1.

transmission of 775 nm laser counter-propagating

775 laser detuning (10 MHz)

Figure 2.1: In counter-propagating case, the relationship between the transmission rate and the detune of the 775nm laser when the 780nm laser is on resonance.

The counter propagating is a nearly Doppler-free case since the wave vector of 2 lasers are almost cancels with each other. In order to prove it is true, we can check the case where the 2 lasers are propagating in the same direction. We just need to change the sign of the wavevector of the one of the lasers (here we choose the 775 nm laser.) The plot is shown in figure 2.2.

From the two figures here we can see that in counter-propagating case, the absorption rate of the 775 nm laser is 6% when the 2 lasers are both on resonance. However, when the 2 lasers are propagating in the same direction and on resonance, the absorption rate of the 775 nm laser reduced to nearly 1.2%. This proves that in the quasi Doppler-free

32

Figure 2.2: In the same direction case, the relationship between the transmission rate and the detune of the 775nm laser when the 780nm laser is on resonance.

case, more atoms are contributing to the absorption. That means it is worthwhile to see how absorption is influenced by the exact Doppler-free situation that can be obtained in a 3-photon excitation.

2.2.3 Estimation of the absorption using a numerical integration

As I mentioned before, we can also use a numerical integration to calculate the absorption of the lasers in this configuration. Here we use the software Mathematica to perform the calculation. One thing to notice is that when solving the simultaneous linear equations, the Mathematica does not support using the function "conjugate" together with the "solve" function. Thus, besides writing out the Eq. 2.63 and have the derivatives equal to 0, we also need to write the density matrix equations for $\tilde{\rho}_{10}, \tilde{\rho}_{21}$ and $\tilde{\rho}_{21}$. Combining the equation $\rho_{00} + \rho_{11} + \rho_{22} = 1$, we have Mathematica solve the ten simultaneous equations.

We first present the result when the 780 nm laser is on resonance and the 775 nm laser is scanning and is probed (noting that the p means probe and the d means detuning in figures in this thesis):
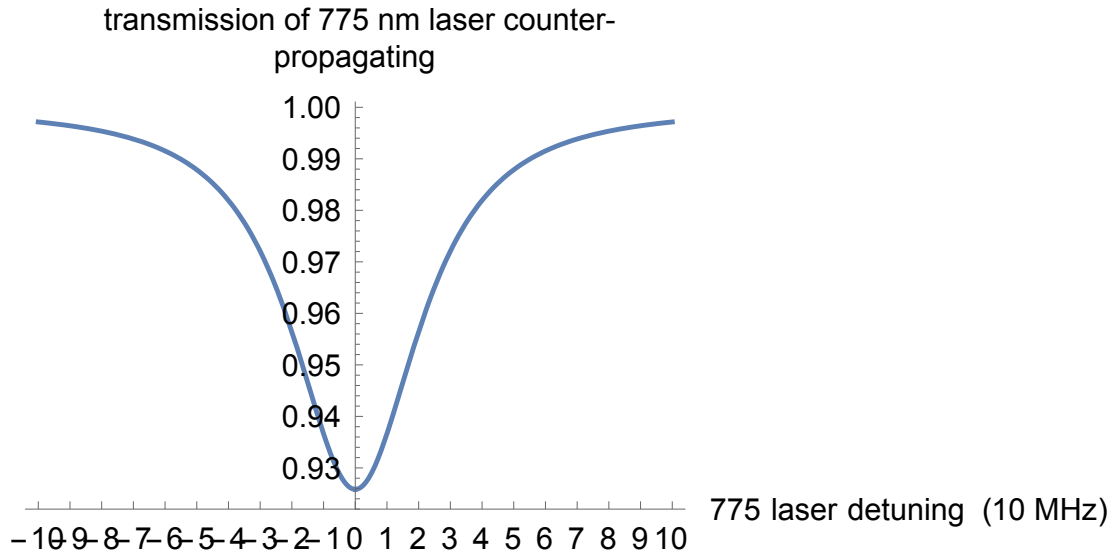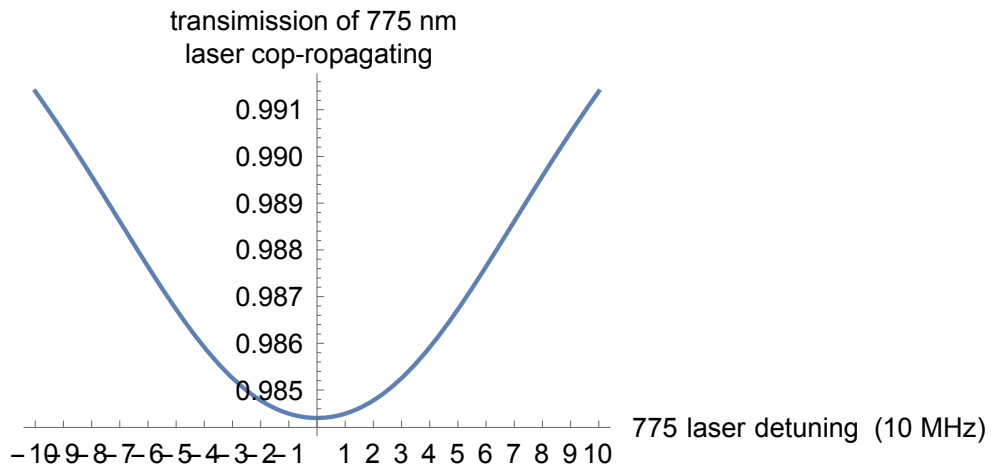
d

Figure 2.3: In the counter-propagating case, the relationship between the transmission of 775 nm laser and the detuning of the 775 nm laser when the 780nm laser is on resonance by numerical method.

Comparing figure 2.1 with figure 2.3, for the counter-propagating case, we can see that when the two lasers are both on resonance, the perturbation method and the numerical method lead to similar absorption, which is around 8%. Besides, the full width at half maximum of the two peaks are both at 50 MHz.

transmission of 775nm laser co-
propagating

Figure 2.4: In the co-propagating case, the relationship between the transmission rate of the 775 nm laser and the detune of the 775 nm laser when the 780nm laser is on resonance by numerical method.

Also, comparing the figure 2.2 and figure 2.4, for the configuration that the 2 lasers are in the same direction, we can see that when the 2 lasers are both on resonance, the 2 methods result in a similar absorption rate, which is around 1.2%. Also, the full width at half maximum for the two peaks are both around 100 MHz.

This means the perturbation method to obtain an analytical solution in valid when we have 775nm in the weak probe condition. Also, the numerical method is proven to be valid to calculate the absorption of both of the 2 lasers under general conditions where the analytical method is not applicable.

Then, the transmission rate of the 780nm laser in both configuration can be calculated from the numerical method. Figure 3.5 and 3.6 show the result.

Figure 2.5: In the counter-propagating case, the relationship between the transmission rate of the 780nm laser and the detune of the 775 nm laser when the 780nm laser is on resonance by numerical method.

From the figure we can see that in both configurations, when the 775 nm laser is closer to resonance, the absorption of the 780 nm laser is suppressed a little. Also, because the intensity of the 775 nm laser is in the weak probe condition, it will affect the absorption of the 780nm laser a little no matter in which configuration.
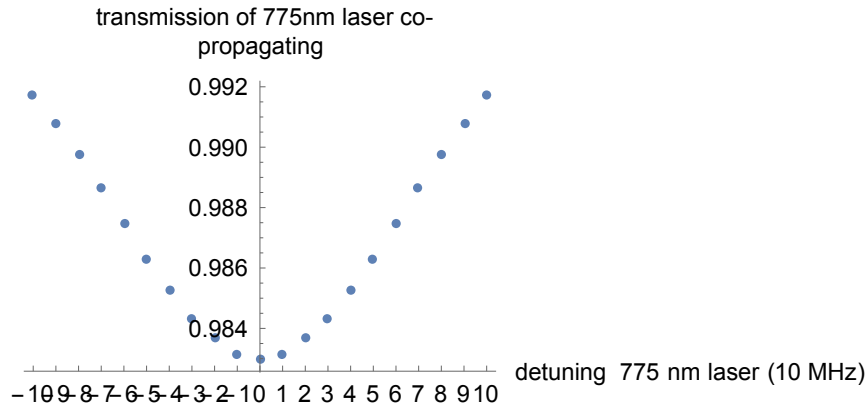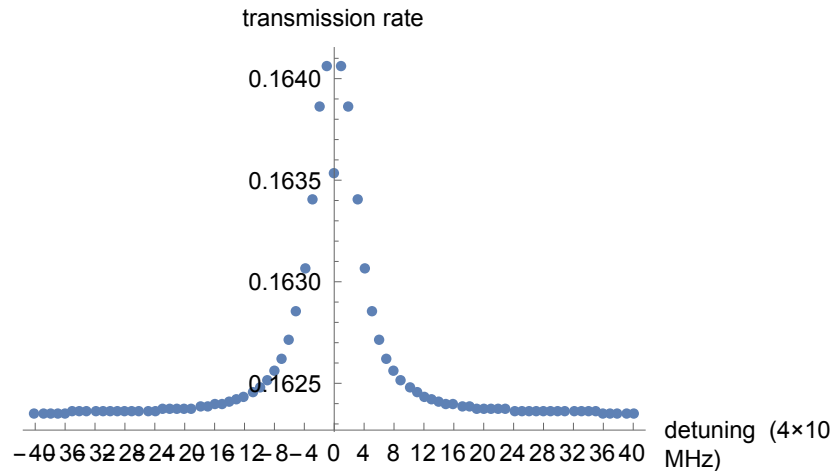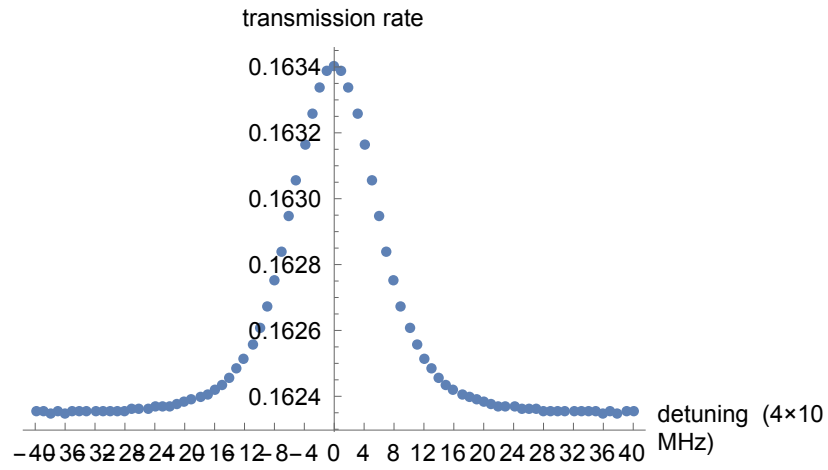
Figure 2.6: In the co-propagating case, the relationship between the transmission rate of the 780 nm laser and the detune of the 775 nm laser when the 780nm laser is on resonance by numerical method.

2.3　Absorption in a 3-photon excitation

In this section, we will come to the final step: exploring the absorption of one of the 3 lasers in the ladder 3-level system for the Rubidium 87 atoms. The first step excitation is performed by the 780 nm laser, exciting the atoms from $5s_{1/2}$ state to $5p_{3/2}$ state. We call it pumping laser. The second step excitation is performed by a 775 nm laser, exciting the atoms from $5p_{3/2}$ state to $5d_{5/2}$ states. We call it probe laser. The last step is performed by the 1260 nm laser. It will excite the atoms from $5d_{5/2}$ state to $50p$ or $50f$ Rydberg states. We call it coupling laser. Since the 1260 nm laser cannot be seen by eyes, it is harder to adjust the alignment. Here we focus on the absorption of the other 2 lasers in this 3-photon excitation. We will look at both the Doppler-free case and the collinear case. The numerical method introduced in last section will be applied here again.

The same as before, we need to construct the density matrix in the field interaction representation. The first step is still writing out the basis in the field interaction representation. Here I choose the basis as:

$$|\tilde{1}(t)> = |1> \tag{2.92a}$$

$$|\tilde{2}(t)> = e^{-i\omega_{pu}t}|2> \tag{2.92b}$$

$$|\tilde{3}(t)> = e^{-i(\omega_{pu}+\omega_{pr})}|3> \tag{2.92c}$$

$$|\tilde{4}(t)> = e^{-i(\omega_{pu}+\omega_{pr}+\omega_c)t}|4> . \tag{2.92d}$$

In this basis, we can again write out $i\hbar\dot{\tilde{\mathbf{c}}} = \tilde{\mathbf{H}}\tilde{\mathbf{c}}$ in order to get the Hamiltonian:

$$\tilde{\mathbf{H}} = \begin{pmatrix} 0 & \frac{\Omega_{pu}}{2} & 0 & 0 \\ \frac{\Omega_{pu}}{2} & \delta_{pu} & \frac{\Omega_{pr}}{2} & 0 \\ 0 & \frac{\Omega_{pr}}{2} & \delta_{pu} + \delta_{pr} & \frac{\Omega_c}{2} \\ 0 & 0 & \frac{\Omega_c}{2} & \delta_{pu} + \delta_{pr} + \delta_c \end{pmatrix}. \tag{2.93}$$

Again, applying the equation (3.28) again, the density matrix equations for this system can be written out:

$$\dot{\rho}_{11} = -\frac{i\Omega_{pu}}{2}(\tilde{\rho}_{21} - \tilde{\rho}_{12}) + \Gamma_2\rho_{22} \tag{2.94a}$$

$$\dot{\rho}_{22} = -\frac{i\Omega_{pu}}{2}(\tilde{\rho}_{12} - \tilde{\rho}_{21}) - \frac{i\Omega_{pr}}{2}(\tilde{\rho}_{32} - \tilde{\rho}_{23}) + \Gamma_3\rho_{33} - \Gamma_2\rho_{22} \tag{2.94b}$$

$$\dot{\rho}_{33} = -\frac{i\Omega_{pr}}{2}(\tilde{\rho}_{23} - \tilde{\rho}_{32}) - \frac{i\Omega_{pr}}{2}(\tilde{\rho}_{43} - \tilde{\rho}_{34}) + \Gamma_4\rho_{33} - \Gamma_3\rho_{22} \tag{2.94c}$$

$$\dot{\rho}_{44} = -\frac{i\Omega_c}{2}(\tilde{\rho}_{34} - \tilde{\rho}_{43}) + \Gamma_4\rho_{44} \tag{2.94d}$$

$$\dot{\tilde{\rho}}_{12} = -\frac{i\Omega_{pu}}{2}(\rho_{22} - \rho_{11}) + \frac{i\Omega_{pr}}{2}\tilde{\rho}_{13} + (i\delta_{pu} - \gamma_{12})\tilde{\rho}_{12} \tag{2.94e}$$

$$\dot{\tilde{\rho}}_{13} = -\frac{i\Omega_{pu}}{2}\tilde{\rho}_{23} + \frac{i\Omega_{pr}}{2}\tilde{\rho}_{12} + \frac{i\Omega_c}{2}\tilde{\rho}_{14} + (i(\delta_{pu} + \delta_{pr}) - \gamma_{13})\tilde{\rho}_{13} \tag{2.94f}$$

$$\dot{\tilde{\rho}}_{14} = -\frac{i\Omega_{pu}}{2}\tilde{\rho}_{24} + \frac{i\Omega_c}{2}\tilde{\rho}_{13} + (i(\delta_{pu} + \delta_{pr} + \delta_c) - \gamma_{14})\tilde{\rho}_{14} \tag{2.94g}$$

$$\dot{\tilde{\rho}}_{23} = -\frac{i\Omega_{pu}}{2}\tilde{\rho}_{13} - \frac{i\Omega_{pr}}{2}(\rho_{33} - \rho_{22}) + \frac{i\Omega_c}{2}\tilde{\rho}_{24} + (i\delta_{pr} - \gamma_{23})\tilde{\rho}_{23} \tag{2.94h}$$

$$\dot{\tilde{\rho}}_{24} = -\frac{i\Omega_{pu}}{2}\tilde{\rho}_{14} - \frac{i\Omega_{pr}}{2}\tilde{\rho}_{34} + \frac{i\Omega_c}{2}\tilde{\rho}_{23} + (i(\delta_{pr} + \delta_c) - \gamma_{24})\tilde{\rho}_{24} \tag{2.94i}$$

$$\dot{\tilde{\rho}}_{34} = -\frac{i\Omega_{pu}}{2}\tilde{\rho}_{34} - \frac{i\Omega_{pr}}{2}(\rho_{44} - \rho_{33}) + (i\delta_c - \gamma_{34})\tilde{\rho}_{34}. \tag{2.94j}$$

The same as the last section, to perform the numerical calculation with Mathematica, we need to write out the another 6 density matrix equations for $\tilde{\rho}_{21}, \tilde{\rho}_{31}, \tilde{\rho}_{41}, \tilde{\rho}_{32}, \tilde{\rho}_{42}$, and

$\tilde{\rho}_{43}$. Then, having all the derivatives equals to 0 and combining the 16 density matrix equations with $\rho_{11} + \rho_{22} + \rho_{33} + \rho_{44} = 1$, we get a set of 17 simultaneous equations to solve.

Before presenting the numerical calculation in Mathematica, there is one thing that should be clarified. In the 3-photon excitation, especially in the Doppler-free configuration, the Doppler shift is not the same way shown in the detuning terms as that in the 2-photon excitation. In figure 3.7, a general spacial distribution is presented:
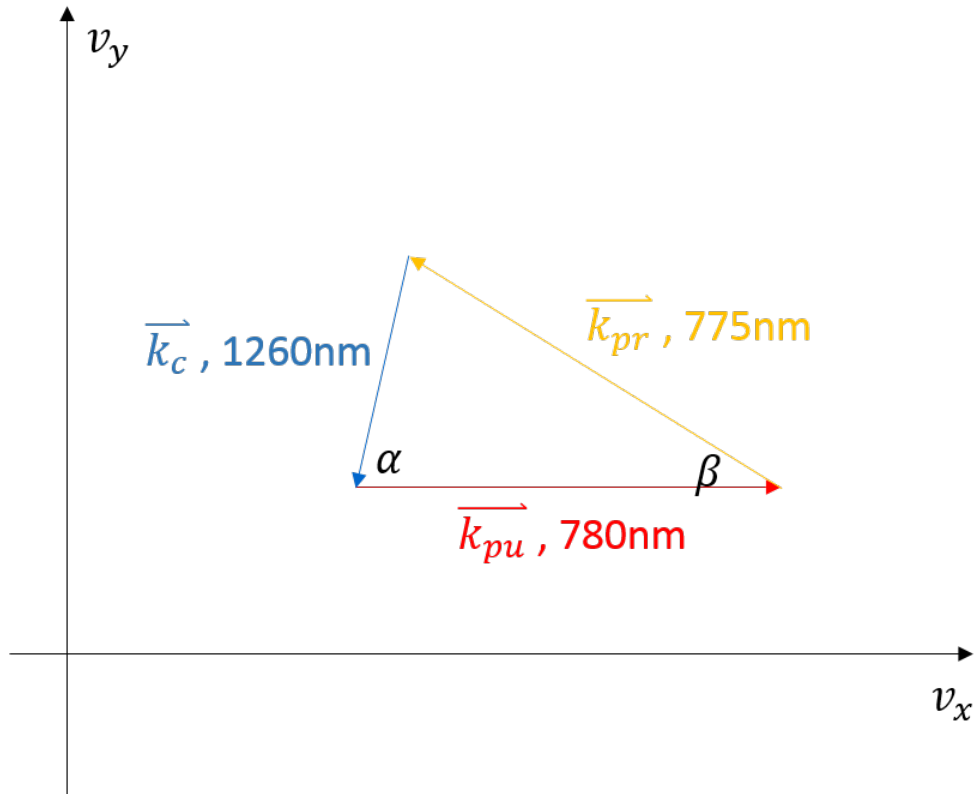

Figure 2.7: A general spatial distribution of 3 lasers

Here α is the angle between 780nm laser and 1260 laser. β shows the angles between the 780 nm laser and 775 nm laser.

In this configuration, the Doppler shift may be accounted for by the replacements:

$$\delta_{pu} \to \delta_{pu} + \vec{k_{pu}} \cdot \vec{v} = \delta_{pu} + k_{pu}v_x \tag{2.95a}$$

$$\delta_{pr} \to \delta_{pr} + \vec{k_{pr}} \cdot \vec{v} = \delta_{pu} - k_{pr}cos(\beta)v_x + k_{pr}sin(\beta)v_y \tag{2.95b}$$

$$\delta_c \to \delta_c + \vec{k_c} \cdot \vec{v} = \delta_c - k_ccos(\alpha)v_x - k_csin(\alpha)v_y. \tag{2.95c}$$

For the collinear configuration, $\alpha = \beta = 0$ (1260 nm laser and 775 nm laser are in the same direction counter-propagating with 780 nm laser).

Notice that the lifetime of Rydberg states is calculate according to Ref. [16]. The lifetime of Rubidium atoms in 50P states is $106\mu s$ and that in 50D states is $294.4\mu s$.

The Rabi frequency of the 1260 nm laser is calculated by Professor James D.D. Martin (here I set the intensity of the 1260 nm laser as $5mW/cm^2$). The transition dipole moment from $5d_{5/2}$ to $50p_{3/2}$ is $0.0132ea_0$ and that between the $5d_{5/2}$ to $50d_{5/2}$ is $0.0022ea_0$.

The calculation performed here takes $5d_{5/2}$ to $50p_{3/2}$ transition as an example.

Then the absorption property can be evaluated by the numerical method.

Figure 2.8: In the collinear configuration, the transmission rate of 780 nm laser when the 780 nm laser is detuned and the other 2 lasers are on resonance.

transmission of 780 nm laser collinear

Figure 2.10: In the collinear configuration, the transmission rate of 780 nm laser when the 1260 nm laser is detuned and the other 2 lasers are on resonance.

transmission of 780nm laser collinear

Figure 2.9: In the collinear configuration, the transmission rate of 780 nm laser when the 775 nm laser is detuned and the other 2 lasers are on resonance.

Figure 2.8 to 2.10 present the absorption of 780 nm laser in collinear configuration when

only one of the lasers are detuned while the other two lasers are on resonance.

transmission of 775 nm laser collinear

Figure 2.11: In the collinear configuration, the transmission rate of 775 nm laser when the 780 nm laser is detuned and the other 2 lasers are on resonance.

transmission of 775 nm laser collinear

Figure 2.12: In the collinear configuration, the transmission rate of 775 nm laser when the 775 nm laser is detuned and the other 2 lasers are on resonance.

transmission of 775 nm laser collinear
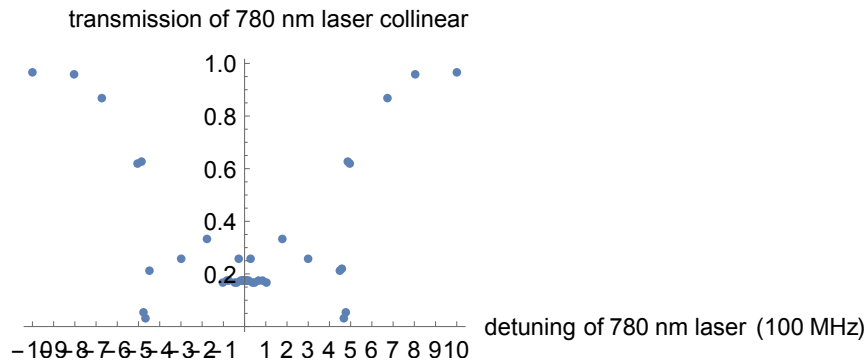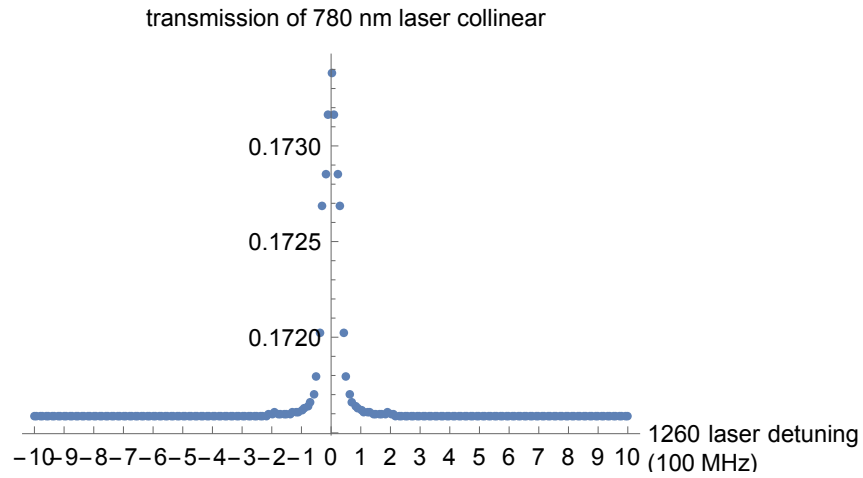

Figure 2.13: In the collinear configuration, the transmission rate of 775 nm laser when the 1260 nm laser is detuned and the other 2 lasers are on resonance.

Figure 2.11 to 2.13 present the absorption of 775 nm laser in collinear configuration when only one of the lasers are detuned while the other two lasers are on resonance.

For Doppler-free configuration (see figure 2.7), the wavevectors of 3 lasers cancel with each other:

$$k_{pu} - k_{pr}cos(\beta) - k_c cos(\alpha) = 0 \qquad (2.96\text{a})$$

$$k_{pr}sin(\beta) - k_c sin(\alpha) = 0 \qquad (2.96\text{b})$$

From these 2 equations we get: $\alpha = 72.6°$ and $\beta = 35.94°$

Then the absorption in the Doppler-free configuration can be presented.

44

transmission of 780 nm laser Doppler-free

Figure 2.14: In the Doppler-free configuration, the transmission rate of 780 nm laser when the 780 nm laser is detuned and the other 2 lasers are on resonance.
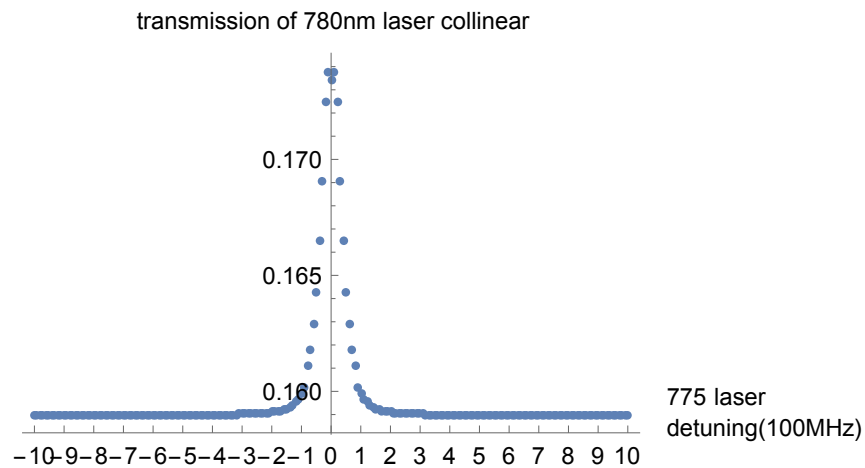
tansmission of 780 nm laser Doppler-free
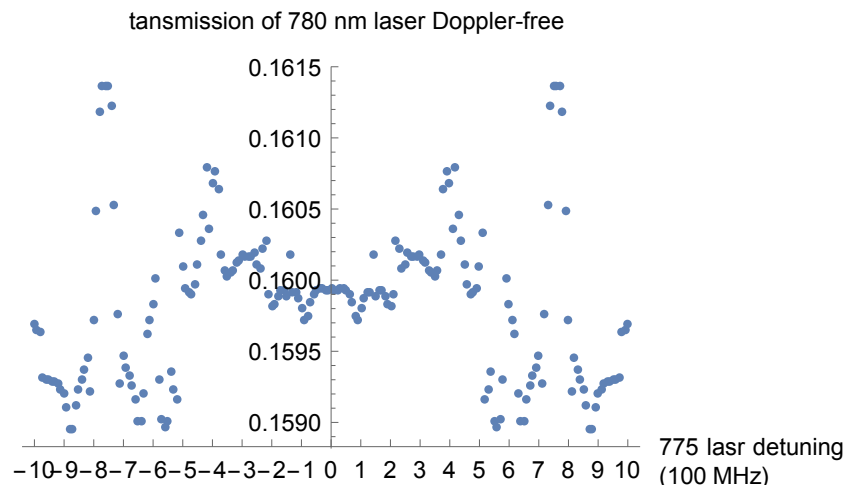
Figure 2.15: In the Doppler-free configuration, the transmission rate of 780 nm laser when the 775 nm laser is detuned and the other 2 lasers are on resonance.

transmission of 780 nm laser Doppler-free

1260 laser detuning (100 MHz)
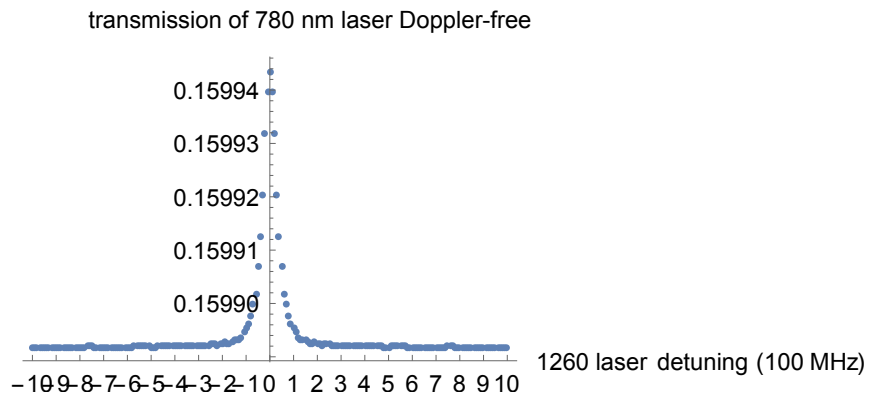
Figure 2.16: In the Doppler-free configuration, the transmission rate of 780 nm laser when the 1260 nm laser is detuned and the other 2 lasers are on resonance.

Figure 2.14 to 2.16 show the absorption of 780 nm laser in the Doppler-free configuration when only one of the lasers are detuned while the other two lasers are on resonance.
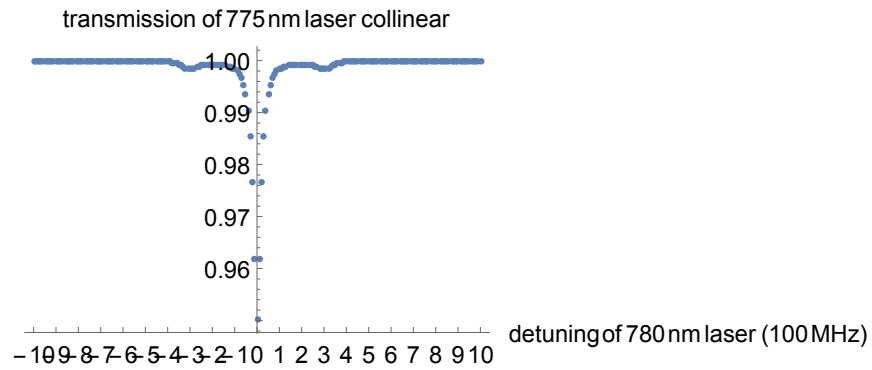

transmission of 775 nm laser Doppler – free

detuning of 780 nm laser (100 MHz)
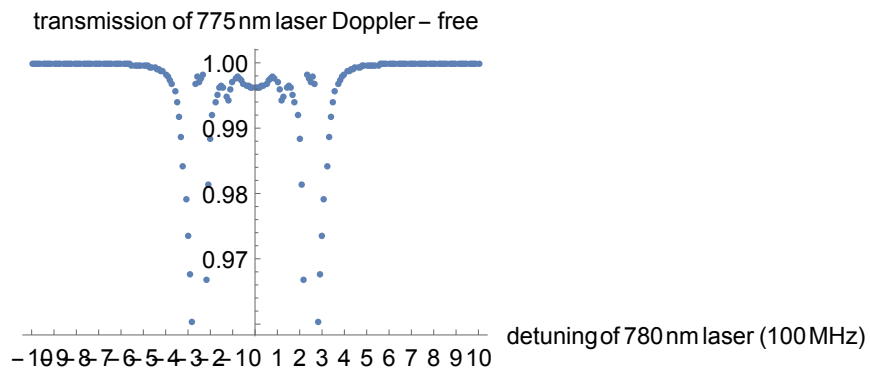
Figure 2.17: In the Doppler-free configuration, the transmission rate of 775 nm laser when the 780 nm laser is detuned and the other 2 lasers are on resonance.
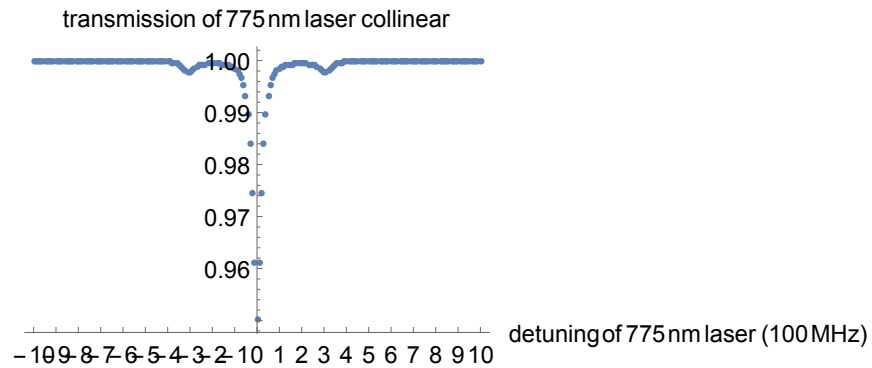
46

transmission of the 775 nm laser Doppler − free
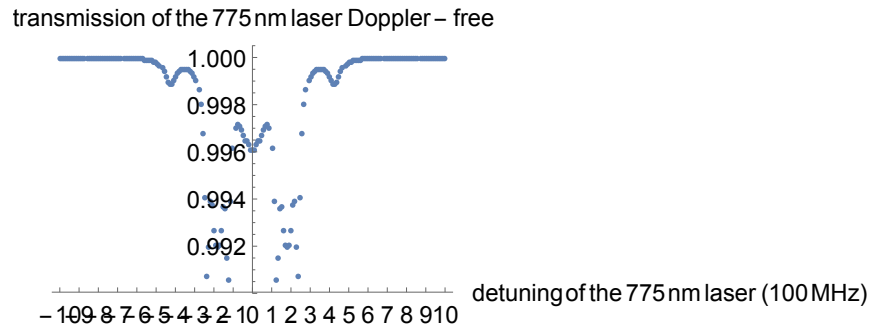
Figure 2.18: In the Doppler-free configuration, the transmission rate of 775 nm laser when the 775 nm laser is detuned and the other 2 lasers are on resonance.
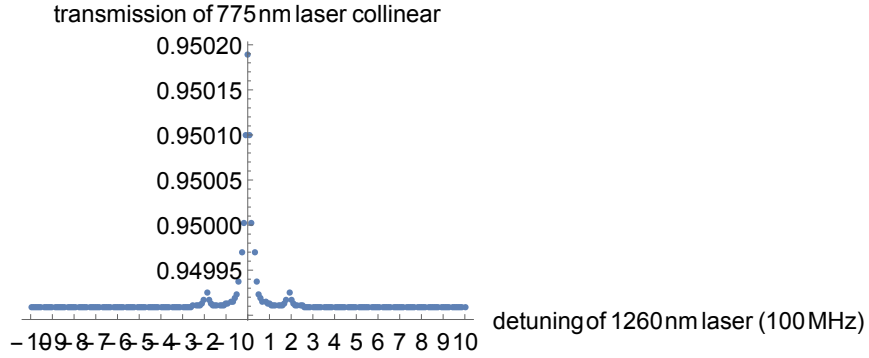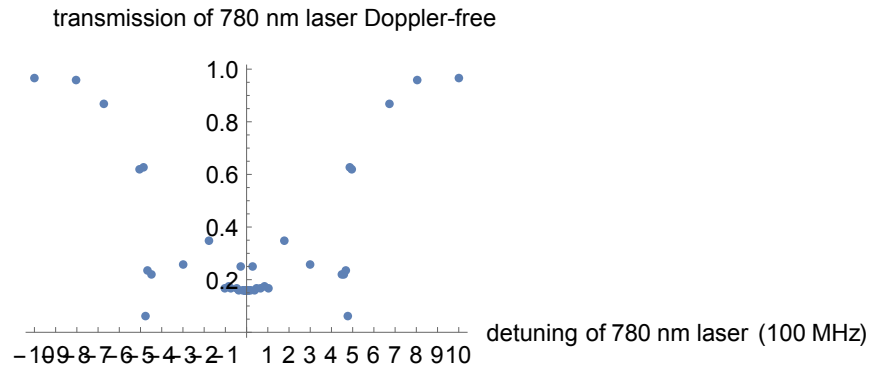

transmission of 775nm laser Doppler− free
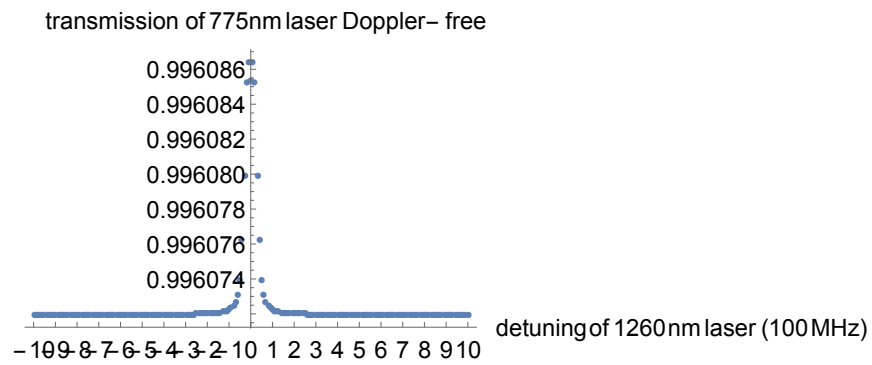
Figure 2.19: In the Doppler-free configuration, the transmission rate of 775 nm laser when the 1260 nm laser is detuned and the other 2 lasers are on resonance.

Figure 2.17 to 2.19 show the absorption of 775 nm laser in the Doppler-free configuration when only one of the lasers are detuned while the other two lasers are on resonance.

To prove the validity of the integration from Mathematica, I plot the imaginary part of the complex susceptibility density vs v_x and v_y when all the 3 lasers are on resonance in the Doppler-free configuration.
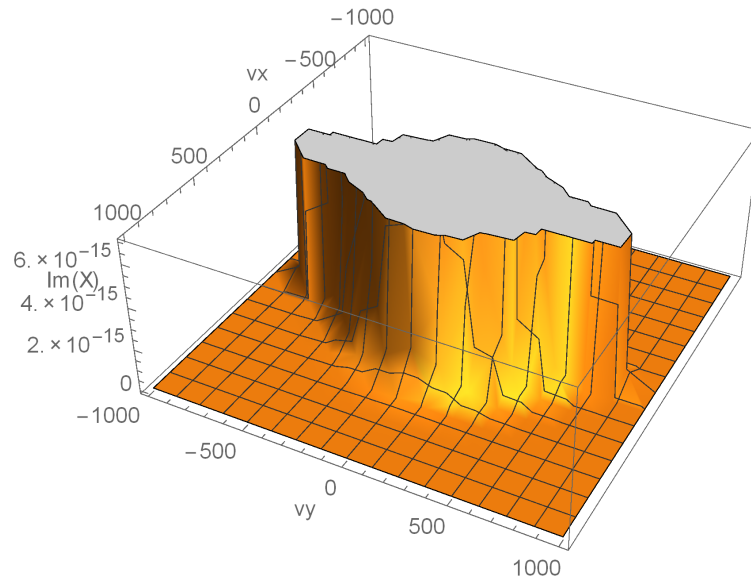
Figure 2.20: $Im[\chi](v_x, v_y)$ vs v_x and v_y in the Doppler-free configuration when 3 lasers are all on resonance(v from -1000 m/s to 1000 m/s)
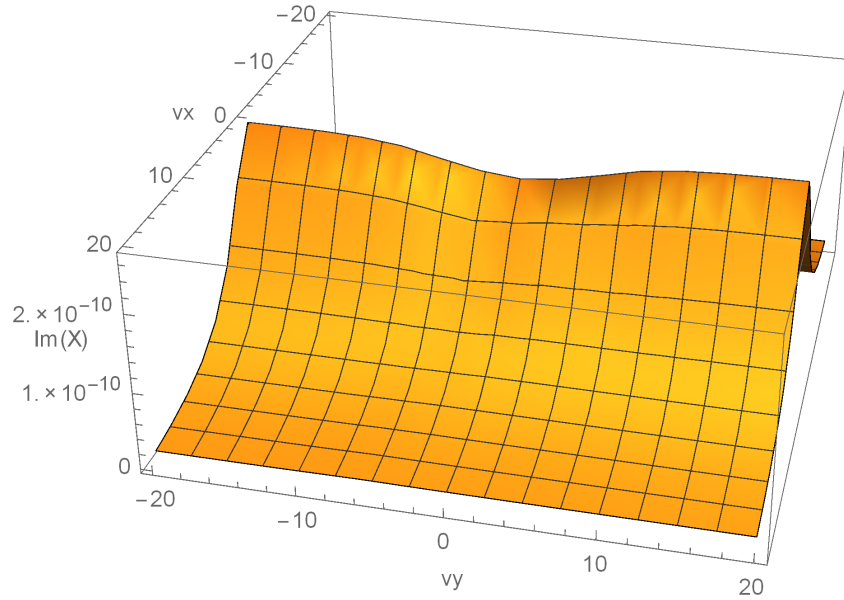
Figure 2.21: $Im[\chi](v_x, v_y)$ vs v_x and v_y in the Doppler-free configuration when 3 lasers are all on resonance (v from -10 m/s to 10 m/s)

Figure 2.20 shows that the imaginary part of the complex susceptibility is a mountain within the 2000 m/s by 2000 m/s velocity range. Figure 2.21 shows the top of the mountain. That means this mountain is with finite height so the integration converges. Also, the form of the imaginary part of the complex susceptibility density is a polynomial of v_x and v_y multiplied by two exponentials $e^{-v_x^2/u^2}$ and $e^{-v_y^2/u^2}$. Since the decreasing speed of the negative exponential is faster than the increasing speed of any polynomial, the integration must converges from the math point of view.

From figure 2.8 to figure 2.19, one conclusion is that in our lab, the 780 nm laser and 775 nm laser are on resonant, if we scan the 1260 nm laser, it is easier for us to detect the absorption of the 780 nm laser since the intensity change of the intensity of 780 nm during the scanning is larger comparing to that of the 775 nm laser in both configurations (Collinear

case: $\Delta I_{780d} = \frac{2}{1000}, \Delta I_{775d} = \frac{1}{4000}$; Doppler-free case: $\Delta I_{780d} = \frac{4}{100000}, \Delta I_{780d} = \frac{3}{250000}$).
One strange phenomenon is that here the Doppler-free configuration does not increase the absorption in the 3-photon excitation compared to that in the collinear configuration. That is possible because the collinear configuration here is a near Doppler- free configuration, the absorption here does not have much space to be improved. What is more, in the three-photon excitation system, when one of the lasers is on resonance, the absorption of other lasers may be suppressed (For example in figure 2.16, when the 1260 nm laser are approaching resonance the absorption of the 780nm laser is suppressed). Doppler-free case is the most ideal configuration for the absorption.It may lead to some more suppression of the absorption of this whole system. However, it seems that the Doppler-free spectroscopy contains more information than that in the collinear one. For example, in Figure 2.11 when scanning the 780 nm laser while the other two lasers are on resonant in the collinear config-uration, the absorption (spectroscopy) of 775 nm laser presents two sidebands besides the center peak and this character is even more apparent in Figure 2.17 showing that situation in Doppler-free configuration. These sidebands may come from Rabi splitting. Some more similar and interesting features are shown in the absorption of the lasers. They may be related to the EIT and EIA effects and can be figured out in the future.

2.4   Conclusion

In this chapter, the theory estimating absorption of lasers by atomic vapor in a 1-photon, 2-photon, and 3-photon excitation system(Rb 87, 780 nm, 775 nm and 1260 nm diode laser) at room temperature is introduced. Absorption of the laser in a 1-photon excitation is evaluated by calculating the absorption cross-section. The result of the estimation here is consistent with what we usually observe in the lab for the 780 nm laser going through

a Rubidium vapor cell. For the 2-photon excitation system, an analytical method and a numerical integration method are introduced here. The calculation is based on the relationship between the complex susceptibility and the density matrix elements. The analytical method developed by Adam's Group in Durham is utilized to verify the self-developed numerical method. The results of the two methods here are consistent with each other, and the result proves a quasi Doppler-free configuration system can increase the absorption of the 775 nm laser. This result encourages me to calculate the absorption of lasers in a 3-photon excitation system in an exact Doppler-free configuration. For the 3-photon excitation system, the idea of calculation is similar to that for a 2-photon excitation system. The important part is to evaluate the 2D integration over the velocity space. The result here shows that when the 1260nm laser is detuned, it is better to detect the 780 nm laser than to detect the 775 nm laser since the absorption of the 780 nm laser is stronger than that of the 775 nm laser. Also, figure 2.11, 2.12, 2.17, and 2.18 shows that the exact Doppler-free configuration can present more insights of the 4-level system compared to a quasi Doppler-free configuration. Also, some phenomena still need more work to be done to obtain a reasonable explanation. For example, the absorption of 780nm and 775 nm laser in an exact Doppler-free configuration is weaker than that in a quasi Doppler-free configuration (collinear configuration). This result shows that it may be hard to experimentally detect the 3-photon excitation system in a Doppler-free configuration since the length of interaction between the lasers and atoms is also set to be 12 cm for the Doppler-free configuration. One possible alignment to increase the interaction length in the lab is shown in the last figure in this Chapter.
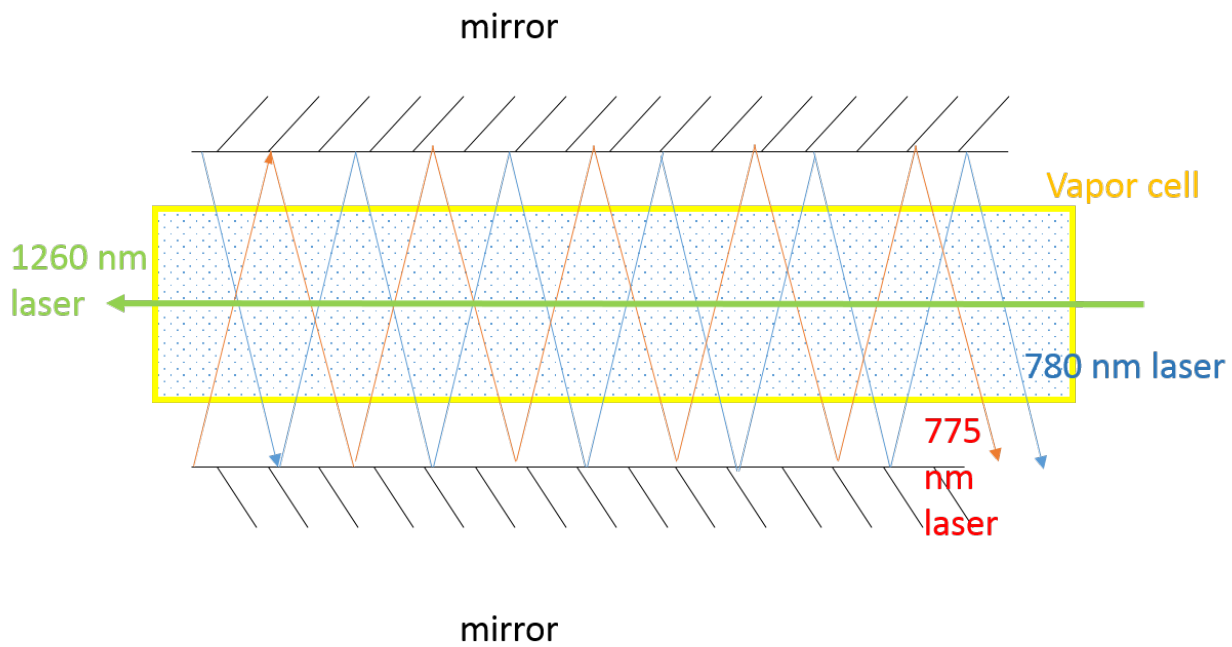
Figure 2.22:   A possible alignment of 3 lasers for the Doppler-free configuration in a room temperature Rb vapor cell.

Chapter 3

Noise Reduction

3.1 Abstract

We need to reduce the noise of the FM signal so that we can have more bandwidth for the feedback system. From doing this, we can get a similar level of signal size by using relatively low laser power.

3.2 Analysis

Figure 3.1 is the configuration of devices for the laser frequency locking system applying frequency modulation techniques. From Figure 3.1 we can see that there is shot noise created at the photodetector and thermal noise produced at the input of all stages of amplifiers. The shot noise and the thermal noise produced before the first stage amplification will be amplified together by the first stage amplifier; however, the noises produced after the amplifier is $\frac{1}{G}$ of the amplified noises, where G is the voltage gain of the first stage

53
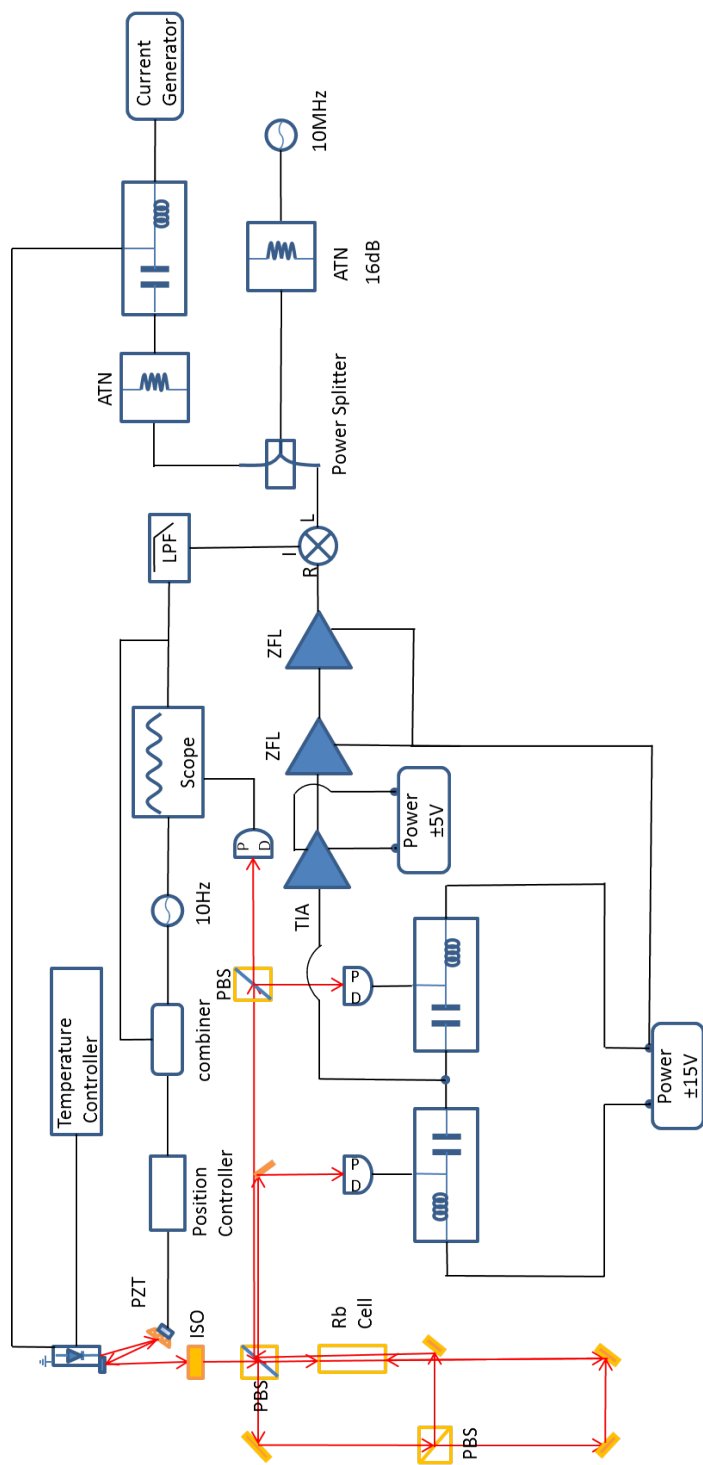
Figure 3.1:   Frequency locking system.

Note: Orange parts are optical devices. Blue parts are electronic devices. Red lines are laser beams

54

amplifier. That means the noise created before the first stage amplification is dominant when we consider the noise in the frequency modulation signal. Formerly in our group, we used the ZFL-500-BNC coaxial amplifier [8] for the first stage amplification. The input impedance of the ZFL-500-BNC amplifier is 50 Ω. The photodetectors detecting the frequency modulation signal are connected to bias tees. The bias tees here will block the dc part of the photocurrent and let the AC part (frequency modulation signal) pass through. The AC current from the photodetector is of the order of $10^{-6}A$ from the measurement. That means a signal of the order of $10^{-4}V$ will be generated. The current noise generated from the photodetector will be amplified with the photocurrent at the same gain. Thus, the value of the input impedance of the amplifier will not affect the current noise size compared with the signal. Meanwhile, the thermal noise created at a resistor is proportional to the square root of its resistance (see Eq. 3.3). Therefore, the larger the input impedance is, the smaller the thermal noise compared with the signal is. For the transimpedance amplifier in my case, the input impedance is 24000 Ω. (The determination of the transimpedance gain will be explained in the next section.) That means the logical structure for the transimpedance amplifier here will decrease the thermal noise compared with the signal size by $\frac{\frac{24000}{\sqrt{24000}}}{\frac{50}{\sqrt{50}}} = 21.98$ times without considering the noise performance of the amplifier itself.

3.3   Description of the transimpedance amplifier

3.3.1   Configuration of a transimpedance amplifier

Figure 3.2 shows a typical design of a transimpedance amplifier that I apply. I choose the input resistance to be 24000 Ω. From Ref. [17], the 3dB bandwidth can be determined by:
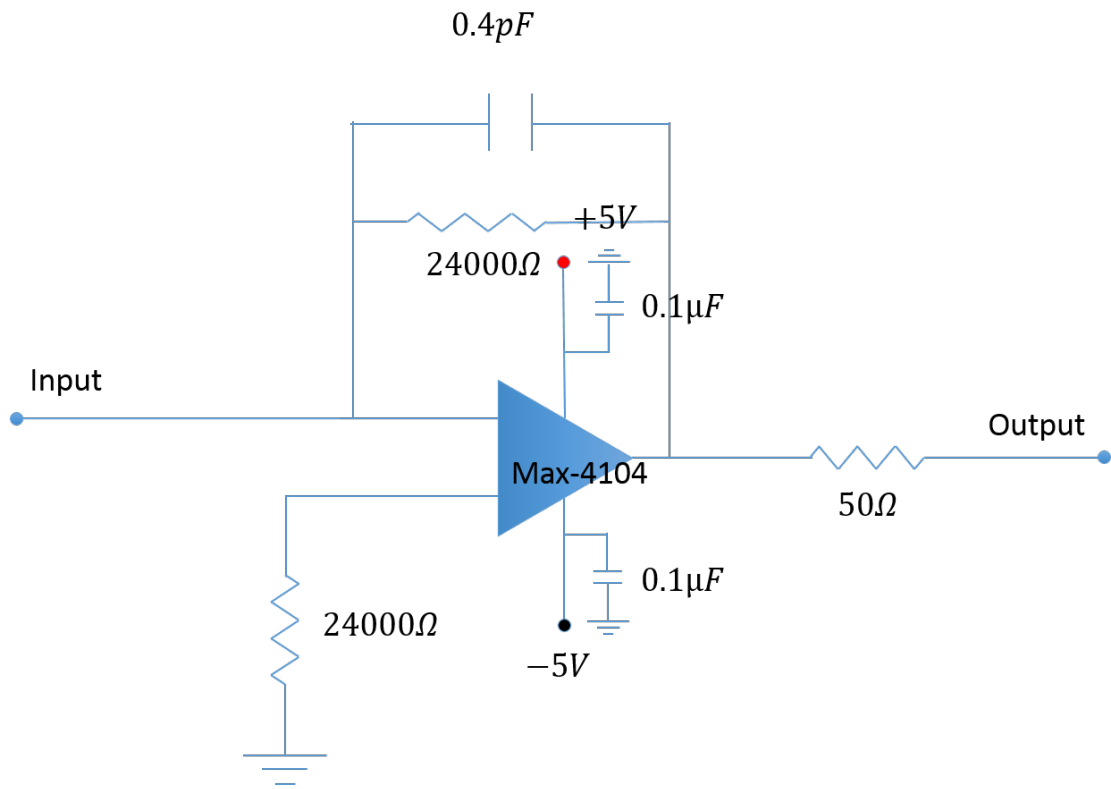
Figure 3.2: A general transimpedance amplifier

$$F_{-3dB} = \sqrt{\frac{GBWP}{2\pi R_F C_S}},\qquad(3.1)$$

where the R_F here is the resistance of the feedback resistor and C_S is the intrinsic capacity of the source (here is the photodetector). $GBWP$ means gain bandwidth product.

In my case, the minimum bandwidth I need is 10MHz (frequency modulation frequency). What is more the existent of a compensation capacitor, which will be introduced later, will decrease the bandwidth of the transimpedance amplifier by some more when we first determine the bandwidth by Eq. 3.1. Therefore, here I first choose the bandwidth to be 20MHz to determine the transimpedance gain (24000 Ω) for stability consideration. The capacitor parallel to the feedback resistor is called compensation capacitor that can prevent the output signal from oscillation. The value of the compensation capacitor can be decided by the formula: $C_F = \frac{1}{4\pi R_F GBWP}(1 + \sqrt{1 + 8\pi R_F C_S GBWP})$ [18]. The role of the resistor at the non-inverting input is to cancel the bias current from the inverting and non-inverting inputs. The two capacitors parallel to the + and - power input are the bypass capacitors that filter out the power supply noise. The 50Ω resistance at the output is utilized to prevent the reflection from the transmission line if there is an impedance mismatch between the transimission line and the next stage device.

3.3.2 Requirements for the op-amp for the transimpedance amplifier

For the modulation of the FM signal is 10 MHz, we need to choose a fast voltage-feedback op-amp with enough Gain Bandwidth Product (the bandwidth of the opamp when the gain is 1 V/V) for frequency response and stability consideration. What is more, to reduce the signal-to-noise ratio of the FM signal, we need to choose an op-amp with low noise density.

Following the guidance of these requirements, 2 op-amps are selected to be the candidates. They are MAX-4104 [19] and OPA-657 [20].

3.4 Noise estimation and comparison

To choose the most suitable op-amp for the transimpedance amplifier, the noise density of the op-comps compared with the ZFL-500-BNC should be estimated. The noise in our system most comes from two main sources: thermal noise and shot noise. The shot noise arises from the randomness of discrete electrons flow (current). The shot noise is most significant in the photo-detection stage, where the photoelectric effect happens. The shot noise density can be calculated by [21]:

$$i_n = (2qI_{dc})^{\frac{1}{2}}, \tag{3.2}$$

where q is the charge of electrons or holes.

The thermal noise is also called Johnson noise. Any resistors no matter if it is connected in a circuit will generate a noise voltage across itself. This noise voltage is just the thermal noise. The thermal noise density can be calculated by [21]:

$$v_{rms} = (4kRT)^{\frac{1}{2}}, \tag{3.3}$$

where k is the Boltzman constant and R is the resistance of the resistor. T is the temperature if the resistor.

Thermal noise and shot noise are white noise source meaning that the noise is uniformly distributed among the frequency domain.

To compare the noise level of the amplifiers, we need to make sure that the noise density is calculated at the same gain because it only makes sense to directly compare the noise based on signals of the same signal level. In what follows, the noise of the ZFL-500-BNC amplifier, as well as the transimpedance amplifier made of the two op-amps will be calculated, and compared with each other.

3.4.1   Noise density of ZFL-500-BNC amplifier

Content in this part is basically following Ref. [1].

Equivalent power added $= (F_1 - 1)kT_0$

Power out $= kT_0G_1 + (F_1 - 1)kT_0G_1 = kT_0F_1G_1$

Equivalent power added $= (F_2 - 1)kT_0$

1   2

2-stage amplifier

X_S

R_S

at T_0

Power out $= (kT_0G_1 F_1)G_2 + (F_2 - 1)kT_0G_2$
$= G_1G_2kT_0[F_1 + (F_2 - 1)/G_1]$
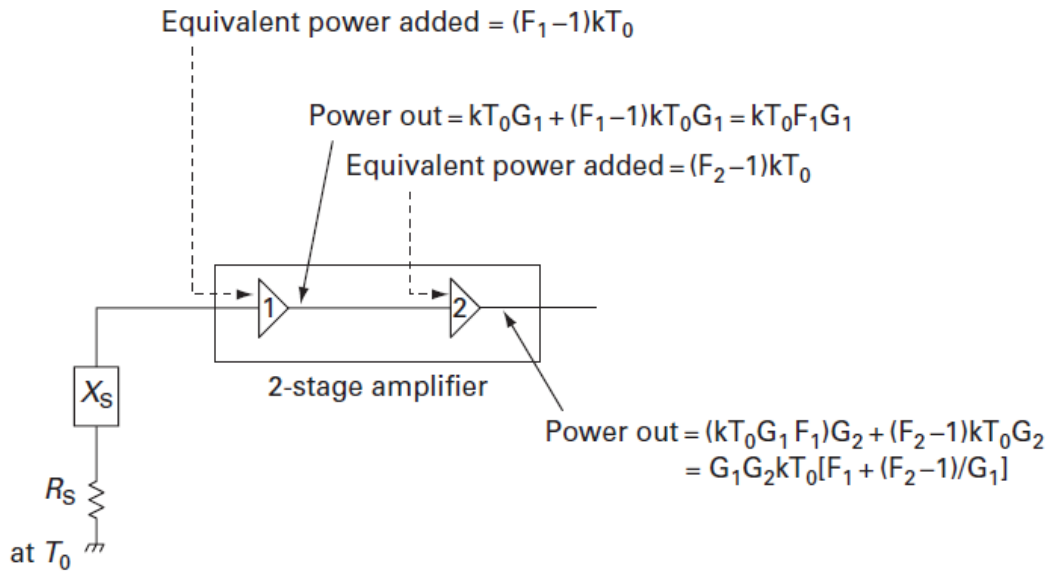
Figure 3.3: A configuration illustrates the relationship between NF and output noise of an amplifier [1]. R_S amd X_S are the source resistance and reactance. k is the Boltzman constant, and T_0 is the temperature of the environment. G_1 and G_2 are the Gains of the two amplifiers. The F_1 and F_2 are the noise factors of the two amplifiers.

From the datasheet of ZFL-500-BNC, we can find the noise figure of the amplifier at 10 MHz is around 5.7 dB. The definition of the noise figure is:

$$NF = 10 \log F. \tag{3.4}$$

where the F, called Noise Factor [1] is defined as:

$$F = \frac{SNR_{in}}{SNR_{out}}. \tag{3.5}$$

Also from the datasheet, the gain of the amplifier at 10 MHz is 22.1 dB, and the definition of the gain is as below:

$$G = P_{out}/P_{in}. \tag{3.6}$$

From Ref. [1], the equivalent noise power (thermal noise density) created from an amplifier is:

$$equivalent\ power\ added = (F_1 - 1)kT_0. \tag{3.7}$$

The noise created before amplification is the shot noise:

$$i_s = \sqrt{2eI_p} = 4.953 \times 10^{-13}\ A/\sqrt{Hz}, \tag{3.8}$$

where I_p is the photocurrent, and the power of this part of noise is:

$$p_s = (i_s)^2 R = 1.227 \times 10^{-23}\ W/Hz. \tag{3.9}$$

From Ref. [1], the power of the noise at the output of the amplifier is:

$$p_o = p_s G + (F - 1)kT_0 G = 1.761 \times 10^{-18} \ W/Hz. \quad (3.10)$$

The T_0 here is the temperature at the input termination and we set it as 290 K.

The noise density represented in voltage is:

$$V_0 = \sqrt{P_0 R} = 9.383 nV/\sqrt{Hz} \quad (3.11)$$

For the gain of the transimpedance amplifier chosen is 24000 Ω, we need to convert the noise density in voltage here to that at the same gain:

$$V_{eo} = V_o \times \frac{24000\Omega}{50\Omega \times G_V} = 354.08 nV/\sqrt{Hz}, \quad (3.12)$$

where $G_V = V_{out}/V_{in}$.

3.4.2   Noise density of the transimpedance amplifiers

The information can be utilized to calculate the noise density of the transimpedance amplifier from the datasheet is the input current noise density and the input voltage noise density. Here we take Max-4104 op-amp as an example and present the noise density calculation result of OPA-657 later on.

The input voltage noise density of Max-4104 is 2.1 $nV/\sqrt{Hz}$ and the input current density is 3.1 $pA/\sqrt{Hz}$.

From Ref. [22] , the noise density from the output of the transimpedance amplifier after amplification can be calculated as:

$$
\begin{aligned}
v_o &= R_F[(v_n/R_F)^2 + (i_n)^2 + (i_s)^2 + 4kT/R_F]^{1/2} \\
&= 24000\Omega \times [(2.1 \times 10^{-9}(V/\sqrt{Hz})/24000\Omega)^2 + (3.1 \times 10^{-12}(A/\sqrt{Hz}))^2 \\
&\quad + (4.953 \times 10^{-13}(A/\sqrt{Hz}))^2 + 4 \times 1.38 \times 10^{-23} J/K \times 290K/24000\Omega]^{1/2} \\
&= 77.88 nV/\sqrt{Hz}.
\end{aligned}
\tag{3.13}
$$

The noise density here is around one fifth of that of the ZFL-500-BNC amplifier.

For OPA-657 op-amp, the typical input noise density at 10MHz is $4.8nV/\sqrt{Hz}$, and the input current density is $1.3fA/\sqrt{Hz}$. Apply the same method determining the transimpedance gain for Max-4104, and here I set the feedback resistor as 56200 Ω. With this information, the output noise density of the transimpedance amplifier can be estimated as:

$$
\begin{aligned}
v_o &= R_F[(v_n/R_F)^2 + (i_n)^2 + (i_s)^2 + 4kT/R_F]^{1/2} \\
&= 56200\Omega \times [1.7 \times 10^{-9}(V/\sqrt{Hz})/56200\Omega)^2 + (2.4 \times 10^{-12}(A/\sqrt{Hz}))^2 \\
&\quad + (4.953 \times 10^{-13}(A/\sqrt{Hz}))^2 + 4 \times 1.38 \times 10^{-23} J/K \times 290K/56200\Omega]^{1/2} \\
&= 41.2 nV/\sqrt{Hz}.
\end{aligned}
\tag{3.14}
$$

For the transimpedance amplifier made of MAX-4104 op-amp, the noise density at the same gain is: $v_o = 77.88nV/\sqrt{Hz} \times \frac{56200}{24000} = 182.37nV/\sqrt{Hz}$.

From theoretical estimation, it seems that OPA-657 op-amp is a more appropriate candidate for the transimpedance amplifier.

3.4.3 Experimental measurement the noise of the amplifiers

In figure 3.1, the IF port the of the mixer is connected to a low pass filter whose -3 dB bandwidth is 3.5 MHz. A mixer mixes an RF input signal with a signal from LO inputs (in

our case is the 10 MHz modulation signal) to create an output signal from the IF output. This output signal consists of 2 frequencies, $F_{LO} + F_{RF}$ and $|F_{LO} - F_{RF}|$. The noise from any frequency domain summed with F_{LO} will be higher than 3.5 MHz and cannot pass the low pass filter. However, the frequency difference between the noise coming from 6.5 MHz to 13.5 MHz and the 10MHz LO input signal will be lower than 3.5 MHz. That means the noise from 6.5 MHz to 13.5MHz will be carried on to the FM signal by the effect of the mixer and the low pass filter. Since the noises calculated here are all white noises, the noise density is the same in any frequency region.

Following is the setup that I use to measure the noise of the ZFL-500-BNC and the two transimpedance amplifiers:
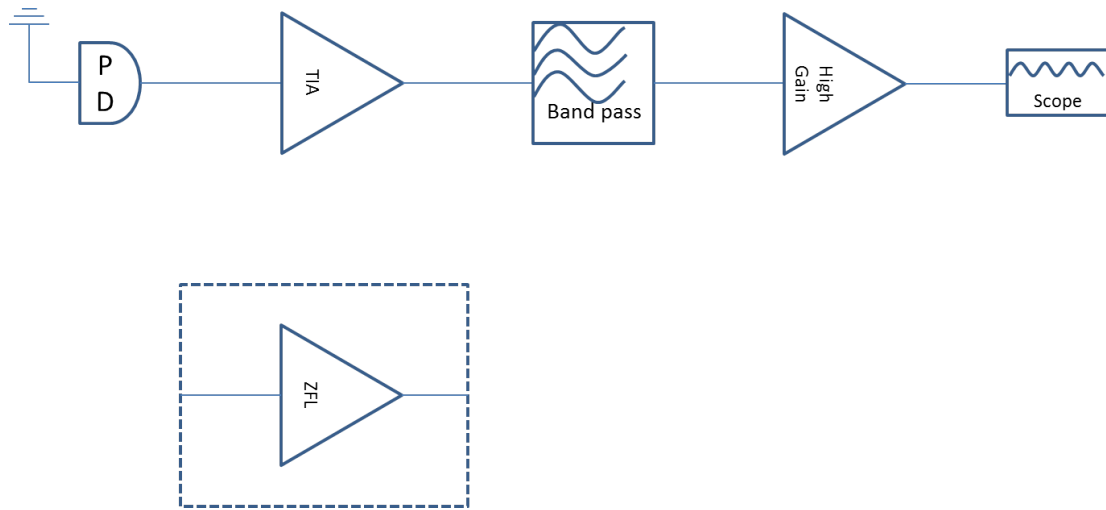

Figure 3.4: Configuration of devices for noise measurement. Here PD means photodetector. TIA means transimpedance amplifier. High gain means a high gain amplifier.

The bandpass filter measures the noise in the 8.9 MHz to 12.7 MHz (3 dB loss) frequency domain. The amplifier after the bandpass filter is a 30 V/V inverting amplifier.

Before performing the measurement, we need to estimate the output signal (noise) size of each amplifier in the measurement setup.

For ZFL-500-BNC, the estimation is as following:

$$
\begin{aligned}
V_o &= v_n \cdot \sqrt{f(3dB)} \cdot G_V \\
&= 9.37 \times 10^{-9} nV/\sqrt{Hz} \times 30 \times \sqrt{3.8 \times 10^6 Hz} \\
&= 0.580 mV.
\end{aligned}
\tag{3.15}
$$

After convert to the same gain of 24000 Ω, the noise size is:

$$
V_o(24000\Omega) = V_o \cdot \frac{24000}{636} = 21.89 mV,
\tag{3.16}
$$

and for the transimpedance amplifier made of MAX-4104 op-amp, the expected noise size is:

$$
\begin{aligned}
V_o &= v_n \cdot \sqrt{f(3dB)} \cdot G_V \\
&= 77.88 \times 10^{-9} nV/\sqrt{Hz} \times 30 \times \sqrt{3.8 \times 10^6 Hz} \\
&= 4.55 mV.
\end{aligned}
\tag{3.17}
$$

Last for the transimpedance amplifier made of OPA-657 op-amp, the estimated output noise size is:

$$
\begin{aligned}
V_o &= v_n \cdot \sqrt{f(3dB)} \cdot G_V \\
&= 41.2 \times 10^{-9} nV/\sqrt{Hz} \times 30 \times \sqrt{3.8 \times 10^6 Hz} \\
&= 2.41 mV.
\end{aligned}
\tag{3.18}
$$

From the estimation, I expect that the lowest noise size will come from the transimpedance amplifier made of OPA-657 op-amp. However, the experimental data shown in Table 3.1 does not fit our expectation. One thing needs to be noticed is that from Ref [21], the rms noise is from $\frac{1}{8}$ to $\frac{1}{6}$ of the peak-to-peak value that we measure from the screen of the oscilloscope. That is where the range of value in row V_{rms} comes from.

Amplifiers	Voltage type	Experimental Result	Expectation Value
ZFL-500-BNC	V_{pp}	3 mV	
	V_{rms}	0.375–0.5 mV	0.580 mV
	to the same G	14.15–18.86 mV	21.89 mV
TIA(MAX-4104)	V_{PP}	20 mV	
	V_{rms}	2.5–3 mV	4.55 mV
TIA(OPA-657)	V_{PP}	50 mV	
	V_{rms}	6.25–8.33 mV	2.41mV

Table 3.1: Comparison of measured and expected noise levels

From Table 3.1, the results of experimental measurement almost fit the expectation value for the first two types of amplifiers. Observation error from the oscilloscope is $\pm 20\%$. Also, the ratio of the noise between the ZFL-500-BNC amplifier and the transimpedance amplifier made of the MAX-4104 op-amp ($\frac{18.86}{3} = 6.29$) fits our expectation ($\frac{21.89}{4.55} = 4.81$), and the noise performance of Max-4104 op-amp is even better than my estimation. The noise of the OPA-657 measured in the experiment is 3 times higher than the estimation value which is also higher than the Max-4104. Thus, we decide to use the Max-4104 op-amp for the transimpedance amplifier.

Besides this two op-amps, I have also tried an op-amp LT6230 [23] from Linear Technology. The situation is similar to that of OPA-657. The noise performance is better than

that of Max-4104 from the datasheet; however, the noise measured from the experiment is higher than that shown on the datasheet.

3.4.4   packaging the circuit into a box

The last step of making this transimpedance amplifier is to package it into a metal box that can isolate the transimpedance amplifier from some of the interference coming from the external environment. To save the -5V power supply, I modify the bipolar transimpedance amplifier to a unipolar one. The modification does not affect the noise performance, which has been checked by experimental measurement. According to the size of the PCB board [24] for the circuit, I choose to use the box HM157-ND from Hammond Manufacturing [25]. To stably put the board into the box, I change the original SMA connectors to longer ones so that I can add washers and nuts on it. Figure 3.5 shows the circuit in the box.
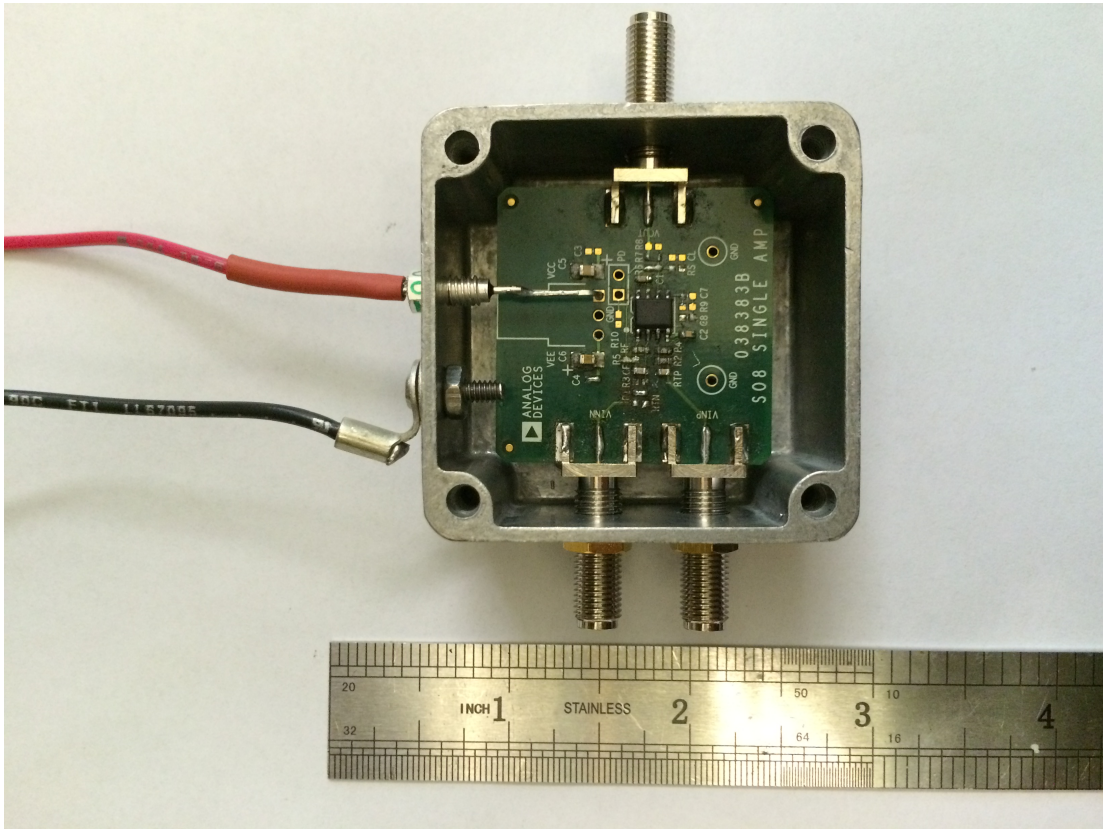
Figure 3.5: A picture indicating how the box is machined and the how the circuit is packaged

3.5   Conclusion

In this chapter, the transimpedance amplifier designed and soldered by myself decreases the noise in the frequency modulation signal by 5 times in power (25 times in voltage). Since part of the laser power is utilized for the frequency locking and this transimpedance amplifier decreases the laser power needed in this part by 5 times, more laser power can be utilized to perform the excitation. What is more, the amplifier can be used to amplify

other AC current signal around 10MHz in the lab.

References

[1] Jon B Hagen. *Radio-frequency electronics*. Cambridge University Press, 1996.

[2] VM Entin, EA Yakshina, DB Tretyakov, II Beterov, and II Ryabtsev. Spectroscopy of the three-photon laser excitation of cold rubidium rydberg atoms in a magneto-optical trap. *Journal of Experimental and Theoretical Physics*, 116(5):721–731, 2013.

[3] II Ryabtsev, II Beterov, DB Tretyakov, VM Entin, and EA Yakshina. Doppler-and recoil-free laser excitation of rydberg states via three-photon transitions. *Physical Review A*, 84(5):053409, 2011.

[4] Pierre Thoumany, Th Germann, T Hänsch, Gernot Stania, Linas Urbonas, and Th Becker. Spectroscopy of rubidium rydberg states with three diode lasers. *Journal of Modern Optics*, 56(18-19):2055–2060, 2009.

[5] Christopher Carr, Monsit Tanasittikosol, Armen Sargsyan, David Sarkisyan, Charles S Adams, and Kevin J Weatherill. Three-photon electromagnetically induced transparency using rydberg states. *Optics letters*, 37(18):3858–3860, 2012.

[6] M Tanasittikosol, C Carr, CS Adams, and KJ Weatherill. Subnatural linewidths in two-photon excited-state spectroscopy. *Physical Review A*, 85(3):033830, 2012.

[7] Mozhgan Torabifard. Transfer cavity stabilization using the pound-drever-hall technique with noise cancellation, 2011.

[8] Mini-Circuits. *Coaxial Amplifier, ZFL-500-BNC*. Rev. B.

[9] Christopher J.Foot. *Atomic Physics*. Oxford University Press, 2013.

[10] Paul R. Berman and Vladimir S. Malinovsky. *Principles of Laser Spectroscopy and Quantum Optics*. Princeton University Press, 2011.

[11] Oregon Center for Optics and Department of Physics, University of Oregon. *Rubidium 87 D line data*, 1 2015. Version 2.1.5.

[12] Timothy T Grove, V Sanchez-Villicana, BC Duncan, S Maleki, and PL Gould. Two-photon two-color diode laser spectroscopy of the rb 5d5/2 state. *Physica Scripta*, 52(3):271, 1995.

[13] Gramham Thiomas Purves. *Absorption And Dispersion in Atomic Vapours: Applications To Interferometery*. PhD thesis, Durham University, Durham, 2006.

[14] Julio Gea-Banacloche, Yong-qing Li, Shao-zheng Jin, and Min Xiao. Electromagnetically induced transparency in ladder-type inhomogeneously broadened media: Theory and experiment. *Phys. Rev. A*, 51:576–584, Jan 1995.

[15] Till Moritz Karbach, Gerhard Raven, and Manuel Schiller. Decay time integrals in neutral meson mixing and their efficient evaluation. *arXiv preprint arXiv:1407.0748*, 2014.

[16] Jongseok Lim, Han-gyeol Lee, and Jaewook Ahn. Review of cold rydberg atoms and their applications. *Journal of the Korean Physical Society*, 63(4):867–876, 2013.

[17] Xavier Ramus. Transimpedance consideration for high-speed amplifiers. Technical report, Texas Instruments, Texas Instruments, Post Office Box 655303 Dallas, Texas 75265, 11 2009.

[18] Wang Tony and Barry Erhman. Compensate transimpedance amplifiers intuitively. Technical report, Texas Instruments, Texas Instruments, Post Office Box 655303 Dallas, Texas 75265, 3 1993. Revised March 2005.

[19] Maxim intergrated. *740MHz, Low Noise, Low Distortion, Op Amps in SOT23-5, Max4104*, 10 1998. Rev.3.

[20] Texas Instrument. *1.6GHz, Low-Noise, FET-Input Operational Amplifier, OPA657*, 10 2001. Rev. F [Revised August 2015].

[21] Paul Horowitz and Winfield Hill. *The art of electronics*. Cambridge University Press, 1989.

[22] Malcolm B Gray, Daniel a Shaddock, Charles C Harb, and Hans-A Bachor. Photodetector designs for low-noise, broadband, and high-power applications. *Review of Scientific Instruments*, 69(11):3755–3762, 1998.

[23] Linear Technology. *215MHz, Rail-to-Rail Output, $1.1nV/\sqrt{Hz}$, 3.5mA Op Amp Family*. Rev. C.

[24] Analog Devices. *8-Lead SOIC Amplifier Evaluation Board User Guide, UG-755*, 2015. Rev.0.

[25] Hammond Manufacturing. *Diecast Aluminum Enclosures, 1590LB*.